Max-Planck-Institut für Meteorologie
Max Planck Institute for Meteorology

Report No. 334

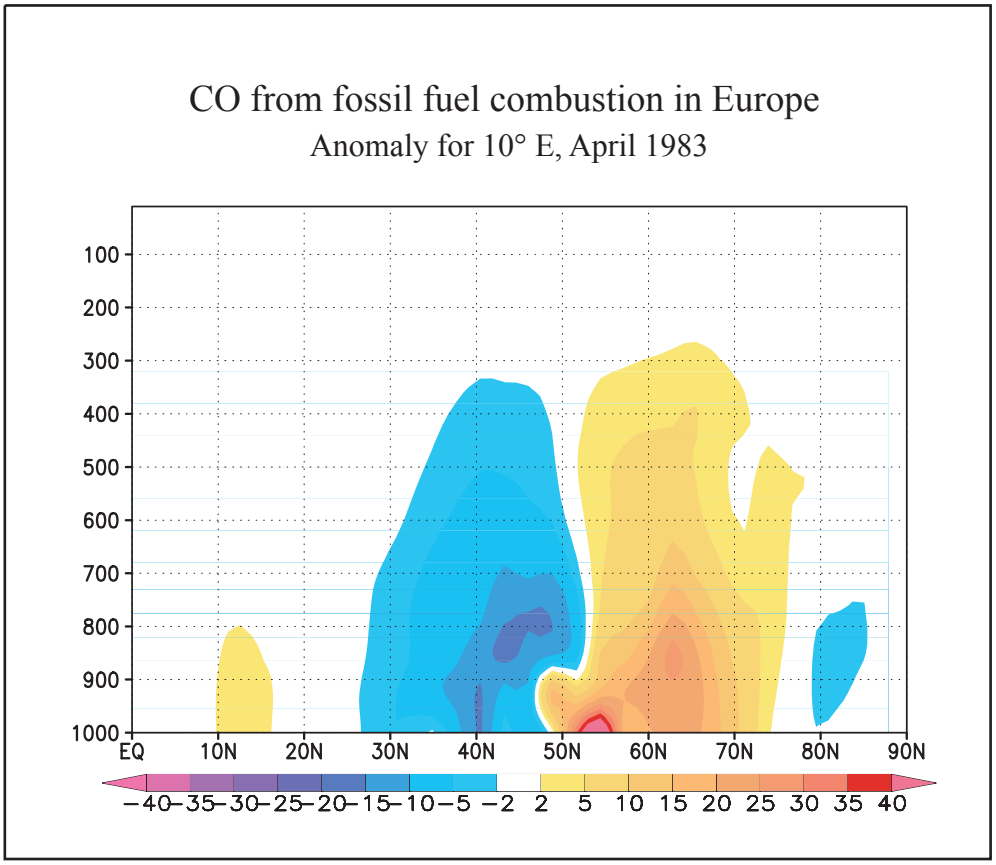

On the Role of European and Non-European Emission Sources for the Budgets of Trace Compounds over Europe

by

Martin G. Schultz • Johann Feichter • Stefan Bauer • Andreas Volz-Thomas

Hamburg, Oktober 2001

Authors

Martin G. Schultz — Max-Planck Institut für Meteorologie
Johann Feichter
Stefan Bauer

Andreas Volz - Thomas — ICG - 2, Forschungszentrum Jülich
Jülich

Max-Planck-Institut für Meteorologie
Max Planck Institute for Meteorology
Bundesstrasse 55
D - 20146 Hamburg
Germany

Tel.:□□ +49-(0)40-4 11 73-0
Fax: +49-(0)40-4 11 73-298
e-mail: <name>@dkrz.de

On the role of European and Non−European Emission Sources for the Budgets of Trace Compounds over Europe

Martin G. Schultz, Johann Feichter, and Stefan Bauer
Max−Planck−Institut für Meteorologie, Hamburg

Andreas Volz−Thomas
ICG−2, Forschungszentrum Jülich

Report of the Max Planck Institute for Meteorology, Hamburg, Germany, No. 334
ISSN 0937−1060

Gleichzeitig Abschlussbericht zum Vorhaben

Beiträge europäischer und aussereuropäischer Quellen zu den Budgets klimarelevanter Spurenstoffe über Europa

BMBF Förderkennzeichen 01 LA 98 325

Gliederung

1.1 Einleitung (german)	3
1.2 Introduction (english)	4
2. Improving current emission inventories	5
3. Numerical simulations of the global distribution of ozone with the MOZART 2 model	7
4. Contributions of european and external emissions to pollutant concentrations over Europe	9
5.1 Summary (english)	13
5.2 Zusammenfassung (deutsch)	15
References/Literaturangaben	17
Figures/Abbildungen	

Kurzzusammenfassung

Das hier beschriebene Forschungsprojekt beschäftigte sich mit einer Analyse des Beitrags europäischer und aussereuropäischer Quellen auf die Konzentration klimarelevanter Spurenstoffe in Europa. Als Modellsubstanz wurde troposphärisches Ozon gewählt. Ein wesentlicher Beitrag des Vorhabens war die Entwicklung zeitabhängiger Emissions−Datensätze mit Hilfe einer einfachen Skalierungsmethode sowie die Weiterentwicklung des globalen Chemie−Transport−Modells MOZART 2, das jetzt der deutschen und internationalen Forschergemeinde zur Verfügung steht. Mit diesem Modell wurde die Ozonverteilung des Jahres 1990 simuliert. Um den Einfluss einzelner Quelltypen und −regionen auf die Schadstoffkonzentration in Europa zu bestimmen, wurde ein Tracer−Markierungsmodell für CO in das globale Zirkulationsmodell ECHAM implementiert. Mit diesem Modell wurde die 15 Jahresperiode 1979−1993 simuliert und die Ergebnisse wurden im Hinblick auf das CO Budget an den Messstationen Izaña, Teneriffa, und Schauinsland, Schwarzwald, analysiert. Rückschlüsse auf das Ozonbudget sind mit diesem Verfahren nur qualitativ möglich.

Abstract

The goal of this study is the analysis of the contribution of European and non−European sources on the budgets of trace gases that are relevant for climate in Europe. Tropospheric ozone was selected as a model substance. Significant contributions from this project were the development of annual emission data sets using a simple scale factor approach, and the participation in the development of the MOZART 2 chemistry transport model, which is now available to the international scientific community. The MOZART 2 model was used to simulate tropospheric ozone for the year 1990. In order to assess the impact of individual source types and −regions, a tagged tracer model for CO was implemented in the general circulation model ECHAM. This model was then used to simulate the 15−year period from 1979 to 1993. The results of this simulation were analysed in terms of the CO budget at the observing stations Izaña, Tenerife, and Schauinsland, Schwarzwald. Implications for the ozone budget at these stations can only be made qualitatively.

1.1 Einleitung

Die Emission von Spurengasen und die Freisetzung von Aerosolen aus anthropogenen und natürlichen Quellen beeinflussen die Lebensqualität der Menschen in Deutschland und Europa auf vielfältige Weise: Zum einen erfolgt eine direkte Schädigung der Gesundheit von Menschen, Tieren und Pflanzen durch die freigesetzten Schadstoffe − insbesondere in Ballungsräumen −, zum anderen werden einige Spurengase in der Atmosphäre durch photochemische Prozesse in toxische Substanzen wie z.B. Ozon umgewandelt, oder sie beeinflussen den Säuregehalt des Niederschlags und führen dadurch zu Schäden an Wäldern und Gebäuden. Einige Spurengase, und insbesondere Aerosole, verändern außerdem die Strahlungseigenschaften der Atmosphäre und tragen daher zum Klimawandel bei.

Das jeweilige Ausmaß der Schädigung wird im wesentlichen durch die Schadstoffdosis (Konzentration · Zeitspanne) bestimmt, oft spielt jedoch auch die Konzentration unmittelbar eine Rolle. In vielen Fällen tritt eine Schädigung erst ein, wenn die Schadstoffkonzentration einen minimalen Schwellenwert für einen bestimmten Zeitraum übersteigt. Andererseits kann bei besonders hohen Schadstoffkonzentrationen auch nach wesentlich kürzerer Zeit eine Schädigung feststellbar sein. In jedem Fall ist es zur Bestimmung des Schadenspotentials einzelner Substanzen und zur Entwicklung geeigneter Gegenmaßnahmen erforderlich, den zeitlichen Verlauf der Spurengas− und Aerosolkonzentrationen möglichst genau zu kennen und Vorhersagen über erhöhte Schadstoffkonzentrationen machen zu können. Aufgrund der vielfältigen Quellen und der wechselseitigen Abhängigkeit verschiedener Spurenstoffe sowie ihrer Ausbreitung durch Transportprozesse, lassen sich solche Vorhersagen nur mit Hilfe komplexer dreidimensionaler numerischer Modelle durchführen, wie sie im Laufe des letzten Jahrzehnts an mehreren Forschungsinstituten in Europa und in den USA entwickelt wurden. Diese Modelle ermöglichen auch eine großflächige systematische Budgetierung einzelner Spurenstoffe und erlauben mit Hilfe einer Markierungstechnik des weiteren die Erstellung quantitativer Zusammenhänge zwischen Emissions− und Immissionsregionen.

Das hier beschriebene Forschungsprojekt verfolgte die folgenden Ziele:

1. Verbesserung bestehender Emissionskataster mit besonderem Augenmerk auf europäische Spurengasquellen
2. Durchführung mehrjähriger numerischer Simulationsrechnungen zur Analyse des Ozonbudgets über Europa
3. Vergleich der Simulationsergebnisse mit Beobachtungsdaten mehrerer deutscher und europäischer Messstationen und Analyse der Repräsentativität dieser Stationen
4. Untersuchung des relativen Anteils europäischer und außereuropäischer Spuren−stoffquellen für die Schadstoffkonzentrationen über Europa

Zusätzlich wurden im Rahmen des Projektes signifikante Entwicklungsarbeiten an dem globalen Chemie−Transportmodell MOZART 2 geleistet, welches nun der inter−nationalen Forschergemeinde für ihre Arbeit zur Verfügung steht.

Dieser Bericht enthält eine Zusammenfassung der Ergebnisse aus den Fragestellungen 1, 2 und 4. Punkt 3 wird in einem gesonderten Bericht beschrieben, der vom Projektpartner MeteorologieConsult GmbH in deutscher Sprache verfasst wurde.

1.2 Introduction

The emissions of trace gases and the release of aerosol compounds from anthropogenic and natural sources influence the quality of life of human beings in Germany, Europe, and elsewhere in a variety of ways: on the one hand humans, animals, and plants are directly affected by the release of pollutant species (notably in urban agglomerations), on the other hand toxic substances, such as ozone, are formed via photochemical processes in the atmosphere. Trace compounds also lead to acidification of rain (with damaging consequences for forests and buildings), or they may alter the radiative properties of the atmosphere and thus contribute to the global climate change.

The amount of damage done by atmospheric pollution is mostly determined by the pollution dose (i.e. concentration times exposure time). On the other hand, the concentrations of the trace compounds often play a direct role as well. For example, it is often noticed that damage occurs only if a certain minimal concentration is exceeded for an extended period of time. In some cases, very high pollutant concentrations can lead to damaging effects much faster than expected. In order to determine the damage potential of specific pollutants and to develop strategies for damage reduction, it is important to obtain a detailed knowledge of the temporal and spatial evolution of traces gases and aerosol compounds, and to be able to predict elevated pollutant concentrations with reasonable accuracy. Due to the multitude of emission sources and because of the feedback processes between various trace compounds and their transport via advection, convection, and diffusion, such predictions are only possible with the help of complex three−dimensional numerical models. These models have been developed at several research institutions in Europe and the US over the past decade. In addition to being useful for tracer predictions, these models also allow for the computation of trace compound budgets on large scales, and they can be used to establish quantitative source−receptor relationships if a tagging technique is applied.

The objectives of the research project 01 LA 98 325, funded by the german ministry for research and education, were:

1. to improve current global trace gas and aerosol emission inventories with a special focus on emissions from Europe
2. to perform multi−annual simulations for the analysis of the budget of ozone over Europe
3. to compare the simulation results with observations from several german and european ground based stations and to analyse the representativeness of these stations
4. to separate the contributions from european and external emission sources to pollutant levels over Europe

Furthermore, the project supported a significant contribution to the development of the global chemistry transport model MOZART 2 which has now become available for the international scientific community.

This report discusses the results obtained in the framework of this project except for the analysis of the observations, which is discussed in a separate document (in German) by the project partner MeteorologieConsult GmbH.

2. Improving current emission inventories

The construction and evaluation of emission inventories for trace gases and aerosol species is a daunting and complex task that requires the collection of a vast amount of data on economical activities and industrial and household processes and their average emission characteristics. The first global inventory of the emissions of several trace compounds was the GEIA inventory [Graedel et al., 1993], which was built under the auspices of the International Global Atmospheric Chemistry Project (IGAC). This inventory contained emission estimates for the year 1985 and it was widely used for atmospheric chemistry modeling studies throughout the 1990s. Since 1996, another emission inventory, EDGAR 2 [Olivier et al., 1996], has been made available. It is based on the year 1990 and contains several improvements and refinements compared to the GEIA inventory. A number of problems have been identified with this inventory, but it still constitutes the state−of−the−art for emission modeling. In recent years, work has been undertaken to build a new version of EDGAR, and this data base is awaiting its release soon.

All of these emission inventories focus on emissions from fossil fuel combustion and industrial processes. Up to now, the important fraction of biomass burning emissions are always estimated according to the coarse resolution inventories by Hao et al. [1994] for tropical forests and savannah, and Ward et al. [1991] for boreal forests. These inventories describe only CO_2 as the dominant emitted species. For other compounds, the models assume that the ratio of emissions of a species X over CO_2 is constant over a wide range of ecosystems and fire conditions. These ratios (so−called emission factors) have been investigated in several field and laboratory studies and there are several compilations of emission factors (c.f. Andreae et al. [2001]).

In addition to these two major categories, several natural processes also release trace gases or aerosol compounds into the atmosphere (e.g. volatile organic compound (VOC) emissions from the terrestrial and marine biosphere, or sulfur emissions from volcanoes). Some inventories exist for such emissions as well, but so far they have remained mostly the effort of individuals rather than being produced by an international consortium.

The global emission data sets are complemented with finer resolution inventories for specific regions. In Europe, the EMEP and CORINAIR projects have compiled such data [e.g. EMEP, 2000], in the US, emissions are routinely estimated by the EPA [e.g. EPA, 1999], and recently, a high−resolution emission inventory for South East Asia has been compiled by Streets et al. [2001].

Except for the EMEP and EPA efforts, no emission inventory so far contains information about the temporal evolution of emissions. The drastic economic changes that have taken place especially since the early 1990s have had a significant impact on the emissions of atmospheric pollutants. For example, emissions of CO, NO_x, and SO_2 from fossil fuel combustion and industrial processes in the former Soviet Union have decreased by about 30%, 30%, and 50%, respectively between 1990 and 1996 [EMEP, 2000]. Even more dramatic are the year−to−year changes in emissions from biomass burning as they become apparent e.g. from studies of the burned area in boreal forests [Wotawa et al., 2001] or from visual inspection of composite images of active fires observed from space [Arino et al., 1996]. So far, global atmospheric chemistry models have made no attempt to take this variability into account.

Within this project we developed a methodology for estimating the relative changes of emissions for individual years based on a simple scale factor approach. A country's emissions from fossil fuel combustion and industrial processes are scaled to the time series of CO_2 emission estimates that is available from the Carbon Dioxide Information Analysis Center (CDIAC). This approach yields reasonable results for countries that have no effective emission control regulations (Figure 1). For countries with pollution control measures, the trends from EMEP and EPA were reviewed and applied. This approach yields emission trend factors for each country relative to a specific base year. In this study, the year 1990 was selected, and the gridded emission data sets from the EDGAR 2 inventory were then scaled with the help of a political map to yield gridded estimates for individual years between 1960 and 1998. Figure 2 provides 3 examples for the scale factor maps produced with this method. It becomes apparent that emissions have increased between 1960 and 1980 in most parts of the midlatitude Northern hemisphere and decreased after about 1990. In contrast, the emissions from many developing countries in the tropical and subtropical regions of both hemispheres have risen continuously so that, by 1995, anthropogenic emissions from China exceeded those from Germany and the former USSR (Figure 3). This shift in the dominant emission regions has important consequences for the composition and chemistry of the global atmosphere. The high levels of UV radiation and water vapour in these regions directly affect the oxidizing capacity of the atmosphere and lead to intensive photochemical production of ozone and other secondary pollutants. The increasing emissions in the tropical areas might also induce significant changes in the Earth's climate through direct release and secondary formation of aerosols.

In order to account for the interannual variability of biomass burning emissions, we used the 5−year time series of active fires detected globally from the ATSR sensor [Arino et al., 1999]. While it is not possible to quantitatively derive emission estimates for biomass burning from the number of active fire pixels detected from space, these data provide at least a semi−quantitative assessment of the large scale variability of biomass burning in space and time. Again, we applied a scale factor approach in order to redistribute the climatological biomass burning emissions from Hao et al. [1994] in time. In this approach, the individual fire locations and dates for each month were first aggregated geographically into the grid boxes of the model and normalized to yield a five−year average of 1 per year for each grid box. The resulting scale factors were then multiplied with the emission fluxes from the standard inventory. Figure 4 shows results from this approach, and Figure 5 compares the interannual variability of the burned area of boreal forest fires in North America and Russia [Wotawa et al., 2001] with the variability of biomass burning emissions resulting from this study. It is seen that the scale factor qualitatively reproduces the interannual variability of burnt area, but underestimates the magnitude of the variations.

3. Numerical simulations of the global distribution of ozone with the MOZART 2 model

The MOZART 2 [Horowitz et al., 2001] model is a global chemistry transport model which has been developed in a collaboration between the National Center of Atmospheric Research (NCAR) in Boulder, the General Fluid Dynamics Laboratory (GFDL) in Princeton, and the Max−Planck Institute for Meteorology (MPI−Met) in Hamburg. The Hamburg version of the model uses meteorological analyses from the European Center for Medium Range Weather Forecast (ECMWF) for the quantification of large−scale advection, and for the parameterisation of unresolved transport in the boundary layer and in convective clouds. The standard resolution is 2.8° x 2.8° with 31 vertical levels extending from the surface to 10 hPa. The chemical scheme consists of 56 advected species with 28 photolysis, 107 gas−phase and 5 heterogeneous reactions, and the time step is 20 minutes.

Surface emissions for carbon monoxide (CO), NO_x, methane (CH_4), ethane, propane, ethene, propene, formaldehyde, acetone, isoprene, terpenes, and other hydrocarbons are prescribed from the EDGAR 2 inventory [Olivier et al., 1996] as monthly averages for the base year 1990 with seasonality from Müller [1992]. Aircraft emissions of NO_x, and CO are taken from Friedl [1997]. A detailed description of the emission data sets used in the MOZART model can be found at *http://acd.ucar.edu/models/MOZART/emissions/emissions.html*.

Within the framework of this study, we performed one simulation with MOZART for the year 1990 and analysed the results with respect to the ozone budget over Europe. A detailed comparison of the MOZART results with observations at several European stations yielded a satisfactory agreement (see separate report of Schmitt [2001]) if the first 1−2 months, where the model is still in its spin−up phase, are omitted from the analysis.

Figures 6 and 7 show monthly mean ozone concentrations for April, July, and October 1990 at the surface, and at 500 hPa. In April, maximum surface ozone concentrations of ~50 ppb occur in the subtropical North Atlantic and in South East Asia with outflow to the Pacific. It has long been recognized [e.g. Duce et al., 1980; Prospero et al., 1985; Merrill et al., 1989a,b] that East Asia constitutes a significant source of pollution which is advected over long distances particularily in spring, when westerlies prevail and photochemistry has not reached its peak intensity. Observations from PEM−West B also indicate mean ozone concentrations greater than 40 ppb in outflow from the East Asian continent [e.g. Talbot et al., 1997] and thus confirm the model results. The cause of the ozone maximum over the North Atlantic is less obvious and contradicts measurements such as those from the mountain station Izaña, Tenerife. There are two possible reasons for this discrepancy: (i) the intensity of biomass burning emissions from North Africa (Sahel zone) is overestimated for April (see also section 4), and (ii) the model overestimates the stratosphere−troposphere exchange of ozone. From a brief analysis of the stratospheric ozone tracer (see below), it appears that over 30 ppb of the 45 ppb of the simulated ozone concentration are of stratospheric origin. Whether this is realistic or a unique feature of the year 1990 remains to be seen in a longer simulation spanning several years.

For July, the MOZART 2 model produces a clear pattern of photochemical ozone production around the major urban centers in the Northern hemisphere with monthly mean maximum concentrations around 60 ppb (greater 70 ppb for the Los Angeles area). The beginning of the burning season in Africa and South America can also be detected with wide−spread, albeit small, increases in ozone over the southern oceans. This signal is much more pronounced in October, when biomass burning in the Southern hemisphere is at its maximum. Peak surface ozone concentrations in South America exceed 70 ppb, in agreement with observations from field experiments such as TRACE−A [Kirchhoff et al., 1996]. Ozone concentrations in Europe are predicted to be as low as 10 ppb at the surface, which is somewhat lower than observed values and points towards an overstimate of the dry deposition sink.

Ozone concentrations in the middle free troposphere (at 500 hPa) also show a clear seasonal cycle. Monthly mean values of more than 70 ppb are predicted for much of the northern hemisphere mid−latitudes. In summer, ozone concentrations are generally higher over Eurasia than over North America, and the maximum ozone concentrations are predicted for the eastern mediterranean region. This is in qualitative agreement with a climatology of ozone sonde data [Logan, 1999], however, the absolute concentrations predicted by the model are too high by about 5−10 ppb. The phenomenon of the Mediterranean ozone maximum is likely caused by advection of ozone that is produced in the source regions of Europe with contributions from lightning NO_x production and East Asian biomass burning [Li et al., 2001]. The ozone enhancement throughout the southern hemisphere, which is seen at the surface, is also evident in the free troposphere. Strong convection near the major biomass burning source regions transports ozone and precursor species into the free troposphere where it can be advected over extremely long distances [e.g. Schultz et al., 1999].

A more quantitative comparison of the seasonal cycle of ozone for the Schauinsland station (8°18’E, 47°55’N, 1205m asl) can be seen in Figure 8. The model generally captures the summer time maximum and the large variability in summertime ozone concentrations, but is has a tendency to overestimate the median concentration. Again, this might be due to an overestimate of the stratosphere−troposphere exchange.

In order to separate the stratospheric ozone contribution from the amount of ozone that is photochemically produced in the troposphere, the MOZART model contains a special tracer O_3S. At each time step, the O_3S concentration for model grid boxes in the stratosphere is reset to the current stratospheric value of ozone. When O_3S is advected downward into the troposphere, it experiences the same loss processes as tropospheric ozone, but it has no photochemical source. Table 1 summarises the stratospheric ozone contribution for the Schauinsland station (model level at 890hPa) as computed from the model. It ranges from 70% in winter to 20% in summer. While the seasonal cycle of this contribution should be relatively well simulated, the absolute values should not be overemphasized. The stratosphere−troposphere exchange (STE) is a notoriously difficult problem in modelling (e.g. [Law et al., 2000]; STE is also the focus of the European STACCATO project). In fact the stratospheric ozone concentrations that are prescribed for the MOZART model had to be reduced by a factor of 2 in order to yield realistic cross−tropopause fluxes.

Month	*Ozone concentration at Schauinsland [ppb]*	*Stratospheric contribution [ppb]*	*Fraction of ozone from the stratosphere*
January*	—	—	—
February	43	30	0.70
March	46	34	0.74
April	48	23	0.48
May	60	22	0.37
June	54	13	0.24
July	57	10	0.18
August	56	11	0.20
September	42	12	0.29
October	38	15	0.39
November	29	16	0.55
December	30	21	0.70

Table 1: Monthly mean ozone concentrations and stratospheric ozone contribution for the station at Schauinsland (8°18'E, 47°55'N, 1205m asl) for 1990 from the MOZART 2 model. No results are given for January because of the model spin−up.

4. Contributions of European and external emissions to pollutant concentrations over Europe

In order to investigate the relative importance of trace gas emissions from Europe and elsewhere on the ozone budget over Europe, one can either use inverse modelling or a technique called "tracer tagging", i.e. a chemical species in the model is replicated several times so that each model tracer corresponds to one specific emission region and/or type. While the former can yield results with a higher level of detail, inverse modeling is extremely demanding in terms of model development and computer time, and for the purpose of this study, the tagging technique is clearly sufficient. Due to the delays in the development of the chemistry transport model MOZART 2, it was not possible within the framework of this study to develop a tagging scheme for ozone itself. Instead we have applied the tagging technique to a module of simplified CO chemistry that can be used with the Hamburg general circulation model ECHAM [Roeckner et al., 1996]. Carbon monoxide is an important precursor species for ozone, it has a reasonably similar lifetime, and its global budget is reasonably well understood [e.g. Novelli et al., 1998]. The analysis of the contribution from different source regions to the CO concentration over Europe can thus potentially serve as a first proxy for the European ozone budget. The CO module is computationally much more efficient than a full model of tropospheric ozone chemistry. It was hence possible to perform a simulation over 15 consecutive years from 1979−1993 using the ERA−15 reanalysis data from ECMWF to "drive" the GCM.

For this purpose, a Newtonian relaxation technique, termed "nudging" is used (first proposed by Krishnamurti et al. [1991]). In this technique, a prognostic variable *A*, which follows the physical dependency *F* is modified by a non−physical term $G\cdot(A_0 - A')$ so that the model approaches a state that is close to the observed quantities A_0:

$$\frac{\partial A}{\partial t} = F(A, \vec{x}, t) + G(A, \vec{x})\cdot(A_0 - A') \qquad (1)$$

The relaxation parameter *G* for each of the four observed quantities divergence, vorticity, temperature, and surface pressure is chosen such that the observed large−scale weather systems are reproduced but smaller−scale phenomena (e.g. convection) are not supressed [Jeuken et al., 1996]. For the purpose of this study, the meteorological reanalyses from the ECMWF serve as observations. They are extracted with a 6−hour time resolution from the MARS archive with a spectral truncation of T42 and vertically interpolated to the 19 vertical levels of the ECHAM model.

The simplified CO chemistry model uses climatological monthly mean OH concentrations from Spivakovsky et al. [2000]. The emission sources for CO are identical to those used in the MOZART 2 model. A globally uniform methane mixing ratio of 1.78 ppm is prescribed, and the production yield of CO from the oxidation of methane by the OH radical is computed explicitely at each time step as well as the sole significant CO loss process (reaction of CO with OH). In order to account for the chemical production of CO from the oxidation of non−methane volatile organic compounds, the MOZART isoprene emissions are instantaneously converted to CO with an assumed yield of 30% in the model. Individual model tracers are defined for total CO, CO from fossil fuel combustion (globally and in three distinct regions, Figure 9), and CO from biomass burning (globally and in five regions, Figure 9).

In the analysis of model results described below, we discarded the first model year (1979) and present results only for 1980−1993. Figures 10−13 show the average global concentration fields of CO and selected individual tagged tracers for the months of January, April, July, and October at the surface, and at 500 hPa. It is evident that northern hemisphere CO concentrations are higher in winter than in summer by a factor of 2 and that the north−south gradient is much weaker during the northern hemisphere summer. The CO concentration generally decreases with altitude, except for a few regions with strong convective acitivity where one encounters a C−shaped profile.

Not surprisingly, the highest CO surface concentrations for the individual tagged tracers are found in the vicinity of the source regions. However, the spread of CO varies considerably between the individual source regions and the season. European emissions dominate over much of the northern high− and midlatitudes, especially in winter. North American emissions exert their maximum influence over the Atlantic region in spring. CO from biomass burning in South East Asia also contributes significantly to the CO concentrations throughout the northern hemisphere in spring, and this source region is the only one in the northern hemisphere to have a significant impact on southern hemisphere CO during (northern hemisphere) summer and fall.

In the middle free troposphere the influence of European emissions is mostly limited to the high northern latitudes while North American CO tends to spread somewhat further south. Locally, the maximum impact of any source region is biomass burning

in South East Asia. Even in a multi−year monthly average, a clear plume−like structure can be observed over the North Pacific, the South East Asian continent, and the Indian Ocean.

Figure 14 compares the model simulations between 1985 and 1993 with measurements from the NOAA CMDL network [Novelli et al., 1992, 1998]. Unfortunately, there is relatively little overlap between the time of the simulations and the observations for most of these stations, but it can be seen that the concentration level and the seasonal amplitude of CO is generally quite well reproduced by the model. For the interpretation of this comparison, it is important to note that the CMDL measurements are explicitely designed to sample clean background air, whereas the model results necessarily represent a mixture of clean and polluted air masses. This difference becomes apparent at a number of stations which are relatively close to local pollution sources, such as Mace Head, Cape Meares, or Wendover. In order to investigate the effect of the CMDL sampling strategy, we reprocessed the observational data and included the samples that were marked as "polluted" in the average. In some cases, this leads to significant improvements. Altogether, the level of agreement between observations and model simulations throughout many regions of he globe is rather encouraging.

According to the time series of Figure 14, the interannual variability of CO exceeds any possible trend for almost all of the stations displayed in spite of significant reductions of CO emissions in the industrialised countries (see section 2). In part, these reductions are compensated for by increasing emissions in developing countries (Figure 2), but even more important is the large contribution of biomass burning emissions, which show large shifts in geographical regions and time from year to year.

The year−to−year variability of CO concentrations over Europe can be seen from Figures 15−18. Here, a vertical cross section of the CO anomalies $(CO-\overline{CO})$ along the 10°E meridian is shown for selected years and the months of January, April, July, and October. Since the variability of emission sources has not been taken into account in this study, and because the OH concentration is the same for each year, the differences seen in Figures 15−18 are solely attributable to variations in the transport patterns. These differences contribute up to 30% of the total CO concentration. As expected, the most significant differences occur for CO from European fossil fuel combustion sources. These sources have the largest impact on the CO concentration in Europe so that relatively small percentage changes already cause a major change in the absolute concentration.

Figure 19 shows time−altitude cross sections for the locations of Izaña (16°W, 28°N, 2360m asl) and Schauinsland (8°18’E, 47°55’N, 1205m asl) for total CO, and Figures 20 and 21 show the seasonal variation of the most important CO tracers for these stations. In spite of the interannual variability discussed above, these plots show a clear seasonal pattern. According to the model, the CO concentration at Izaña is dominated year−round by contributions from biomass burning while fossil fuel combustion contributes only about half of the amount from the former source, and methane oxidation contributes about one third of the total. The highest CO concentrations are predicted for late spring (April−May), and the model attributes those to biomass burning sources in Africa and South East Asia. While biomass burning in South East Asia is indeed near maximum during these months, the satellite

images of active fires indicate that African fires should be almost absent, contrary to the standard inventory after Hao et al. [1994]. Without the contributions from African fires, CO measured at Izaña in spring would be lower by about 10 ppb on average, and by up to 30 ppb during individual pollution episodes (Figure 22). The effect seems large enough that it should be possible to resolve this issue with the help of measurements, i.e. a suite of non−methane hydrocarbon species specific for biomass burning and fossil fuel sources (for example the species pair C_2Cl_4 and $CHBr_3$), which should be analysed in terms of large−scale advection patterns, e.g. with the help of air parcel trajectories.

The maximum impact of fossil fuel combustion on the predicted CO concentration at Izaña occurs in spring, and a secondary maximum is seen in December (Figure ***). Sources in Europe and sources in North America contribute about equal amounts to these maxima (~10−20 ppb). The seasonal cycle of CO from European sources is a little more pronounced than that of CO from North American sources.

For the Schauinsland station, the model indicates a somewhat different source contribution and a higher interannual variability (Figure 21). As one might expect, the major contribution to the CO concentration at Schauinsland stems from European fossil fuel combustion. However, biomass burning sources have an impact that is only about 20% less, and they dominate the CO concentration in the upper troposphere. The comparison of individual years suggests that differences in the vertical exchange are responsible for the large differences seen in the CO concentrations (an increase in the lowest model levels is usually accompanied by a decrease in the upper levels and vice versa), but further analysis is required before a firm statement can be made in this respect. The seasonal cycle of CO at Schauinsland is roughly similar to that at Izaña with maximum concentrations in spring and minimum concentrations in summer. Because of the closer vicinity of the European fossil fuel combustion source, the seasonal variation of fossil fuel CO is more pronounced than that of biomass burning CO, where the dominant sources are farther away. Long−range transport of fossil fuel emissions from North America is the single−most important factor of the non−local pollution sources at Schauinsland in spring (up to 30 ppb), but compared to the absolute concentration level of ~200 ppb during this time of year, America still contributes only about 15% to the total. However, the situation changes above about 5 km altitude: here the contributions from Europe and North America are roughly equivalent, and both are lower than the impact of biomass burning in South East Asia.

An interesting aspect of the model results for Schauinsland is the relatively large contribution of North American biomass burning to the CO concentration near the ground in September/October. This coincides with a seasonal minimum of biomass burning CO from African and South East Asian sources, and the amount of 20−30 ppb also exceeds the contribution from North American fossil fuel combustion. Given the large interannual variability of biomass burning intensity in Canada and the US [Wotawa et al., 2001], it may be possible to detect this signal if measurements of suitable hydrocarbons would be made and analysed with respect to their biomass burning signature and their region of origin as indicated by trajectory calculations.

5.1 Summary

The research project described in this report has led to significant advances in the capacities for global atmospheric chemistry modeling in Germany through participation in the development of the MOZART 2 model and the development of a scale factor approach to construct time−dependent data sets for emissions of CO, NO_x, and other species for individual years. The MOZART 2 model has been successfully applied for a simulation of tropospheric ozone and ozone precursor species for the year 1990. The results from this simulation are encouraging, but problems have been identified with the stratosphere−troposphere exchange, which is an important factor for the ozone budget over Europe. In order to analyse the contribution from individual source regions and types on pollutant concentrations in Europe, we have built a simple CO chemistry model which allows tagging of tracers and uses prescribed OH concentrations for efficient computation over long time intervals. A 15−year simulation has been performed with this model using the ERA−15 reanalysis data from ECMWF to achieve realistic meteorological conditions. The comparison of model results with data from the CMDL measurement stations show good agreement for many stations throughout the entire latitude range. Because the emissions and the OH concentrations for this simulation were repeated from year to year, the model results can be used to determine the influence of changing weather patterns, i.e. transport, on the interannual variability of CO in Europe. It has been found that variations of up to 30% can occur for individual stations, and that most of the variability is caused by changes in the meteorology near the sources.

What can we learn from the tagged CO tracer simulations for the budget of ozone over Europe? The seasonal variation of the two compounds is quite different: CO has its concentration maximum in winter/spring, whereas the ozone maximum near the surface typically occurs in spring/summer. The increased photochemical activity in summer leads to a net loss of CO, while ozone production is effectively increased at that time. Yet another difference is due to the additional ozone source in the stratosphere and the additional sink of ozone by deposition at the surface. Therefore, one can at best hope for some qualitative insights:

(1) The CO concentration in Europe is mostly determined by regional sources but has significant contributions from fossil fuel combustion in North America and biomass burning in South East Asia.

(2) The impact of external sources on the CO concentration in Europe is largest in winter and spring and has a minimum in summer. This minimum is caused by a combination of two factors: (i) higher OH concentrations lead to faster degradation of CO, and thus the background level is reduced, and (ii) the average transport time from the source regions to Europe increases in summer.

(3) Since photochemical activity generally leads to net tropospheric ozone production in the northern hemisphere, the background ozone level is higher in summer than in winter. Previous studies have shown that most ozone production takes place in the vicinity of the sources, and that free tropospheric ozone concentrations are roughly maintained over long distances [e.g. Logan, 1985, Schultz et al., 1998]. Therefore, the influence of external sources on the summertime ozone concentrations in Europe will be larger and more diffuse than for CO [Schmitt et al., 1997].

(4) In winter, when photochemical activity is low in the northern hemisphere, both

species can be treated as passive tracers as a first approximation. Thus, what has been said about the dominant source regions for CO (European fossil fuel combustion, North American fossil fuel combustion and biomass burning in South East Asia) should also apply for ozone. However, because of the additional ozone input from the stratosphere, we can only make a statement about a fraction of the total observed ozone concentration, namely the amount of ozone that was produced in the troposphere itself. Since the MOZART results presented in section 3 indicate that up to 70% of wintertime ozone originates from the stratosphere, it is pointless to attempt more than a qualitative statement here.

Acknowledgements

The authors would like to thank the BMBF for funding the project, and the ECMWF and DWD for providing ample computing time on the ECMWF machines. Stacy Walters and Larry Horowitz stand out in the team of MOZART developers, and Claire Granier must be mentioned for the preparation of emission data. The ECHAM developers under Erich Roeckner also deserve great credit, in particular Ingo Kirchner for implementing the nudging technique. We thank the CMDL Carbon Cycle laboratory for making the long−term monitoring data set available, and Kashif Butt and Katja Winger for preparing many of the plots.

5.2 Zusammenfassung

Ein wesentliches Ergebniss dieses Forschungsvorhabens in technischer Hinsicht stellt die Übernahme des globalen Chemiemodells MOZART 2 und der damit einhergehende enge Austausch zwischen amerikanischen und deutschen Gruppen dar. Erhebliche Fortschritte wurden bei der Aufbereitung von Emissionsinventaren erzielt, indem aufgrund der sogenannten Skalierungsmethode mit nicht allzu grossem Aufwand die Quellstärken einzelner Jahre bestimmt werden können. Mit MOZART 2 wurden die raum−zeitlichen Verteilungen von Ozon− und Ozonvorläufersubstanzen für das Jahr 1990 berechnet. Die Übereinstimmung zwischen Berechnungen und Beobachtungen sind ermutigend. Wie bei allen gröber auflösenden Modellen ist der Austausch zwischen Stratosphäre und Troposphäre nur unvollkommen simuliert. Da dieser Prozess aber zu einem guten Teil die Ozonwerte in der Troposphäre kontrolliert, sind Aussagen zur Herkunft der über Europa befindlichen Ozonsäule mit Unsicherheiten behaftet.

Um die Beiträge einzelner Quellen zu den Schadstoffbudgets über Europa zu bestimmen sowie ein Verständnis der interannuellen Variabilität zu erhalten, wurden Modellexperimente mit nach Quellregionen markierten CO−Tracern durchgeführt. Es wurden die Jahre 1979−1993 simuliert, wobei das globale Zirkulationsmodell der Atmosphäre ECHAM mit den ERA−15 Reanalysen des ECMWF angetrieben wurde, um die beobachtete Meteorologie widerzugeben. Da bei diesen Modellrechnungen die Oxidantienverteilung und die Quellstärken von Jahr zu Jahr nicht variierten, geben die interannuellen Unterschiede in den CO Tracerverteilungen den Einfluss des von Jahr zu Jahr variablen Wetters wider. Diese durch Unterschiede in der Meteorologie verursachten Änderungen betragen an manchen Stationen bis zu 30% und sind überwiegend durch die Witterung nahe den Quellen beeinflusst.

Was haben wir durch diese Experimente bezüglich der Herkunft von Ozon über Europa gelernt?

Die Saisonalität der beiden Spezies CO und O3 sind unterschiedlich: CO weist die höchsten bodennahen Konzentrationen im Winter und Frühjahr auf, während Ozon das Maximum im Frühjahr und Sommer hat. Die gegen Sommer hin zunehmende Oxidationskraft der Atmosphäre führt zu erhöhtem Abbau von CO und zu einer Zunahme der Ozonproduktion. Desweiteren unterscheiden sich die beiden Spezies aufgrund ihrer sehr unterschiedlichen Depositionsrate am Boden und der Bedeutung von Beiträgen aus der Stratosphäre. Folgende Erkenntnisse wurden aus den Modellrechnungen gewonnen:

(1) CO Konzentrationen über Europa sind im wesentlichen durch lokale Quellen bestimmt. Der Gebrauch fossiler Brennstoffe in Nord−Amerika sowie die Verbrennung von Biomasse in Südost Asien leisten ebenfalls einen nicht unerheblichen Beitrag zum CO Budget.

(2) Der Einfluss weiter entfernter Quellen auf die CO Budgets über Europa ist im Winter und Frühjahr am größten und im Sommer am geringsten. Dieses Sommerminimum hat zwei Ursachen: (i) höhere OH Konzentrationen führen zu rascherem Abbau von CO und damit zu einer niedrigeren Hintergrundkonzentration, und (ii) die charakteristische Transportzeit von den Quellregionen nach Europa ist länger.

(3) Da die photochemische Aktivität im Sommer höher ist und damit die Produktion

von Ozon zunimmt, sind die Hintergrundswerte von Ozon in der Nordhemisphäre im Sommer auf einem höheren Niveau als im Winter. Frühere Studien haben gezeigt, dass Ozon überwiegend nahe den Quellen der Vorläufersubstanzen gebildet wird und dass Ozon in der freien Troposphäre relativ lange verweilt [z.B. Logan, 1985, Schultz et al., 1998]. Daher kann man annehmen, dass der Einfluss entfernterer Quellgebiete für Ozon eine wichtigere Rolle als für CO spielt [Schmitt et al., 1997].

(4) Im borealen Winter, wenn die photochemischen Prozesse unbedeutend sind, sind beide Spezies relativ inert und können über weitere Distanzen transportiert werden. Daher sollten die Ergebnisse der CO Simulationen (Einfluss von Verbrennung fossiler Energieträger in Europa und Nord−Amerika, Biomassenverbrennung in Südost Asien) auch auf Ozon übertragbar sein. Da wir den Transport von Ozon aus der Stratosphäre nicht mit hinreichender Genauigkeit quantifizieren können, ist es nur möglich Aussagen bzgl. des Anteils des Ozons zu machen, welches in der Troposphäre gebildet wurde. Allerdings scheint eine Quantifizierung einzelner Quellterme hier wenig sinnvoll, da der Stratosphärenanteil gemäss den MOZART Simulationen bei 70% liegt.

References/Literaturangaben

Andreae, M.O., and P. Merlet, Emission of trace gases and aerosols from biomass burning, Global Biogeochem. Cyc., in press, 2001.

Arino, O., and J−M. Rosaz, 1997 and 1998 World ATSR Fire Atlas using ERS−2 ATSR−2 Data, Proceedings of the Joint Fire Science Conference, Boise, 15−17 June 1999. (http://shark1.esrin.esa.it/ionia/FIRE/)

Duce, R.A., C.K. Unni, B.J. Ray, J.M. Prospero, and J.T. Merrill, Long−range atmospheric transport of soil dust from Asia to the tropical North Pacific: Temporal variability, Science, 209, 1522−1524, 1980.

EMEP, 2000: Vestreng, V., and E. Støren, Analysis of UNECE/EMEP Emission Data, DNMI research note 37, Det Norske Meteorologiske Institutt, July 2000.

Friedl, R. (Ed.), Atmospheric effects of subsonic aircraft: Interim assessment report of the advanced sub−sonic technology program, NASA Ref. Publ. 1400, 143 pp., 1997.

Graedel, T.F., T.S. Bates, A.F. Bouman, D. Cunnold, J. Dignon, I. Fung, D.J. Jacob, B.K., Lamb, J.A. Logan, G. Marland, P. Middleton, J.M. Pacyna, M. Placet, and C. Veldt, A compilation of inventories of emissions to the atmosphere, Global Biogeochem. Cycles, 7, 1−26, 1993.

Hao, W.M., and M.H. Liu, Spatial and temporal distribution of tropical biomass burning, Global Biogeochem. Cyc., 8 (4), 495−503, 1994.

Horowitz, L.W., S. Walters, Denise L. Mauzerall, Louisa K. Emmons, Phil J. Rasch, Claire Granier, Xuexi Tie, Jean−François Lamarque, Martin Schultz, Guy P. Brasseur, A global simulation of tropospheric ozone and related tracers: Description and evaluation of MOZART, version 2, to be submitted to J. Geophys. Res., 2001.

Jeuken, A.B.M., P.C. Siegmund, L.C. Heijboer, J. Feichter and L. Bengtsson: The use of four dimensional data assimilation in a global climate model for the purpose of model validation, J. Geophys. Res. 101, 16,939−16,950, 1996.

Kirchhoff, V.W.J., and P.C. Alvalá, Overview of an aircraft expedition into the Brazilian cerrado for the observation of atmospheric trace gases, J. Geophys. Res., 101 (D19), 23973−23981, 1996.

Krishnamurti, T.N., J.S. Xue, H.S. Bedi, et al., Physical initialisation for numerical weather prediction over the tropics, Tellus A 43(4), 53−81, 1991.

Law, K., P−H. Plantevin, V. Thouret, A. Marenco, W.A.H. Asman, M. Lawrence, P. Crutzen, J−F. Muller, D. Hauglustaine and M. Kanakidou, Comparison between Global Chemistry Transport Model Results and Measurement of Ozone and Water Vapour by Airbus In−Service Aircraft (MOZAIC) Data, J. Geophys. Res., 105, 1503−1525, 2000.

Li, Q.B., D.J. Jacob, J.A. Logan, I. Bey, R.M. Yantosca, H.Y. Liu, R.V. Martin, A.M. Fiore, B.D. Field, B.N. Duncan, V. Thouret, A tropospheric ozone maximum over the Middle East, Geophys. Res. Lett., 28(17), 3235−3238, 2001.

Measurement of Ozone and Water Vapour by Airbus In−Service Aircraft (MOZAIC) Data, J. Geophys. Res., 105, 1503−1525, 2000.

Logan, J.A., Tropospheric ozone: seasonal behaviour, trends, and anthropogenic influence, J. Geophys. Res., 90, 463−482, 1985.

Logan J.A., An analysis of ozonesonde data for the troposphere: Recommendations for testing 3−D models and development of a gridded climatology for tropospheric ozone, J. Geophys. Res., 104 /D13, 16115−16149, 1999.

Merrill, J.T., Atmospheric long−range transport to the Pacific ocean, in: Chemical Oceonography, ed. by J.P. Riley and R. Duce, pp 15−50, Academic, San Diego, Calif., 1989a.

Merrill, J.T., M. Uematsu, and R. Bleck, Meteorological analysis of long−range transport of mineral aerosols over the North Pacific, J. Geophys. Res., 94, 8584−8598, 1989b.

Müller, J.F., Geographical distribution and seasonal variation of surface emissions and deposition velocities of atmospheric trace gases, J. Geophys. Res., 97, 3787−3804, 1992.

Novelli, P.C., L.P. Steele, and P.P. Tans, Mixing ratios of carbon monoxide in the troposphere, J. Geophys. Res., 97, 20,731−20,750, 1992.

Novelli, P.C., K.A. Masarie, and P.M. Lang, Distributions and recent changes of carbon monoxide in the lower troposphere, J. Geophys. Res., 103(D15), 19015−19033, 1998.

Prospero, J.M., D. Savoie, R.T. Nees, R.A. Duce, and J.T. Merrill, Particulate sulfate and nitrate in the boundary layer over the North Pacific ocean, J. Geophys. Res., 90, 10586−10596, 1985.

Olivier, J.G.J., A.F. Bouwman, C.W.M. van der Maas, J.J.M. Berdowski, C. Veldt, J.P.J. Bloos, A.J.H. Visschedeijk, P.Y.J. Zandveld, and J.L. Haverlag, Description of EDGAR Version 2.0, RIVM report 771060 002, TNO−MEP report R96/119, Bilthoven, NL, 1996.

Roeckner, E., K. Arpe, L. Bengtsson, M. Christoph, M. Claussen, L. Dümenil, M. Esch, M. Giorgetta, U. Schlese, U. Schulzweida, The atmospheric general circulation model ECHAM−4: Model description and simulation of present−day climate, MPI−Met. report, Hamburg, Germany, 1996.

Schmitt, R., A. VolzThomas, Climatology of ozone, PAN, CO, and NMHC in the free troposphere over the southern north Atlantic, J. Atmos. Chem., 28 (1−3), 245−262, 1997.

Schmitt, R., Vergleich zwischen Messung und Modellrechnung (MOZART) für Ozon über dem europäischen Kontinent, Abschlussbericht zum Vorhaben 01 LA 9832/5 des BMBF, 2001.

Schultz, M., R. Schmitt, K. Thomas, A. Volz−Thomas, Photochemical box modeling of long−range transport from North America to Tenerife during the North Atlantic Regional Experiment (NARE) 1993, J. Geophys. Res., 103 (D11), 13477−13488, 1998.

Schultz, M.G., et al. (17 co−authors), On the origin of tropospheric ozone and NOx over the tropical South Pacific, J. Geophys. Res., 104 (D5), 5829−5843, 1999.

Spivakovsky, C.M., J.A. Logan, S.A. Montzka, et al., Three−dimensional climatological distribution of tropospheric OH: Update and evaluation, J. Geophys. Res., 105 (D7), 8931−8980, 2000.

Talbot, R.W., et al. (16 co−authors), Chemical characteristics of continental outflow from Asia to the troposphere over the western Pacific ocean during February−March 1994: Results from PEM−West B, J. Geophys. Res., 102/D23, 28255−28274, 1997.

Ward, D.E., and C.C. Hardy, Smoke emissions from wildland fires, Environemtn International, 17 (2−3), 117−134, 1991.

Wotawa, G., P. Novelli, M. Trainer, and C. Granier, Inter−annual variability of summertime CO concentrations in the Northern Hemisphere explained by boreal forest fires in North America and Russia, Geophys. Res. Lett., in press, 2001.

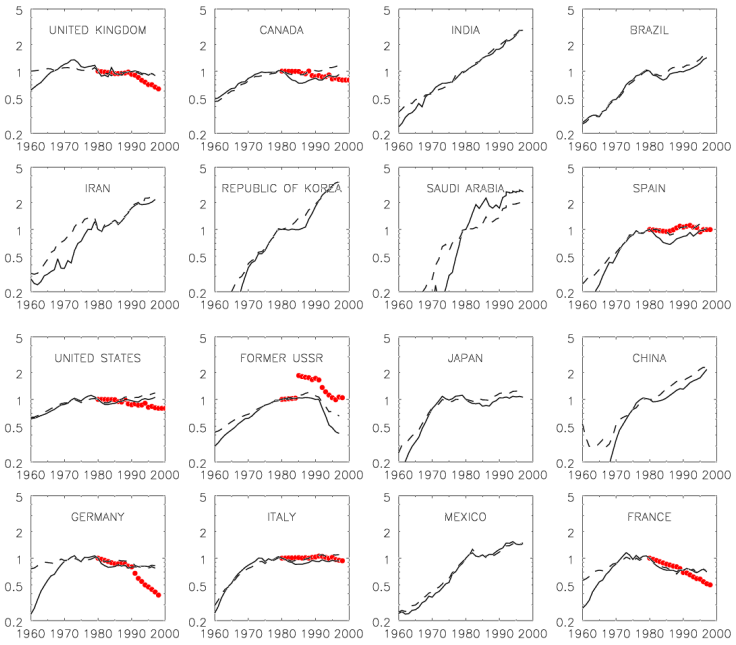

Figure 1: Relative change of liquid fuel CO_2 emissions (solid line), total CO_2 emissions (dashed lines), and CO emissions (red dots) for selected countries in different regions of the world. The CO_2 emission data is from the CDIAC web site, the CO emission data from EMEP [2000].

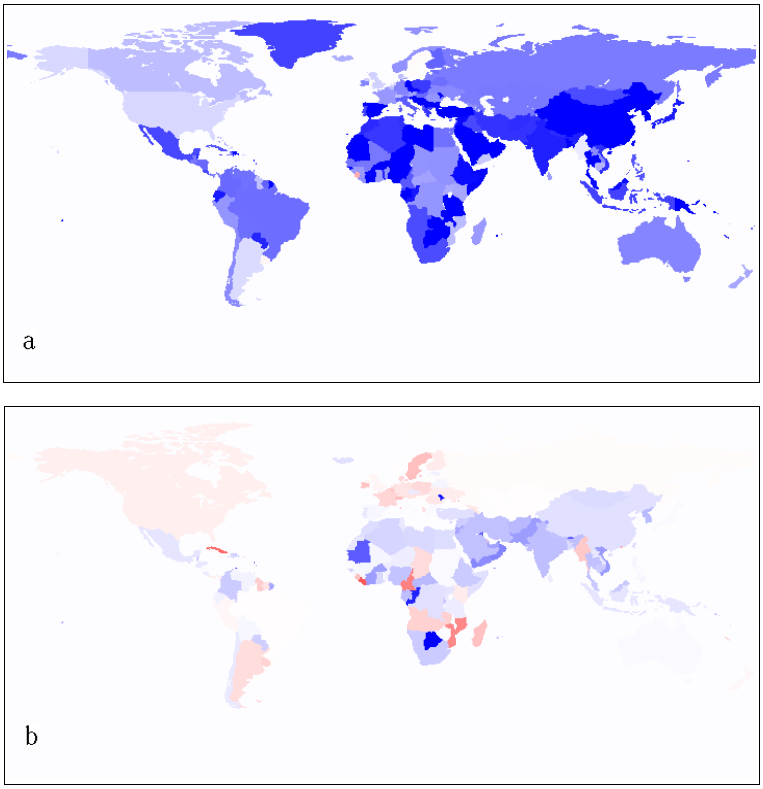

Figure 2: Scale factor maps for CO emissions from fossil fuel combustion and industrial processes for 1960 (a), 1980 (b), and 1998 (c) relative to 1990, the reference year of the EDGAR 2 inventory. Colour scale on next page.

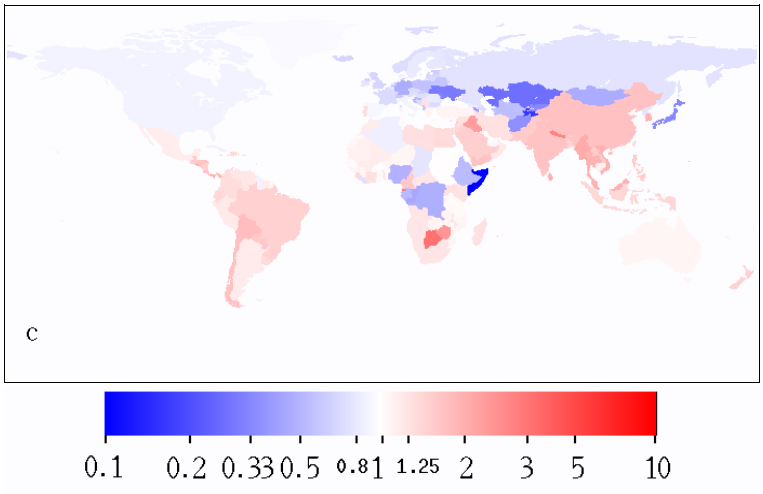

Figure 2 (continued).

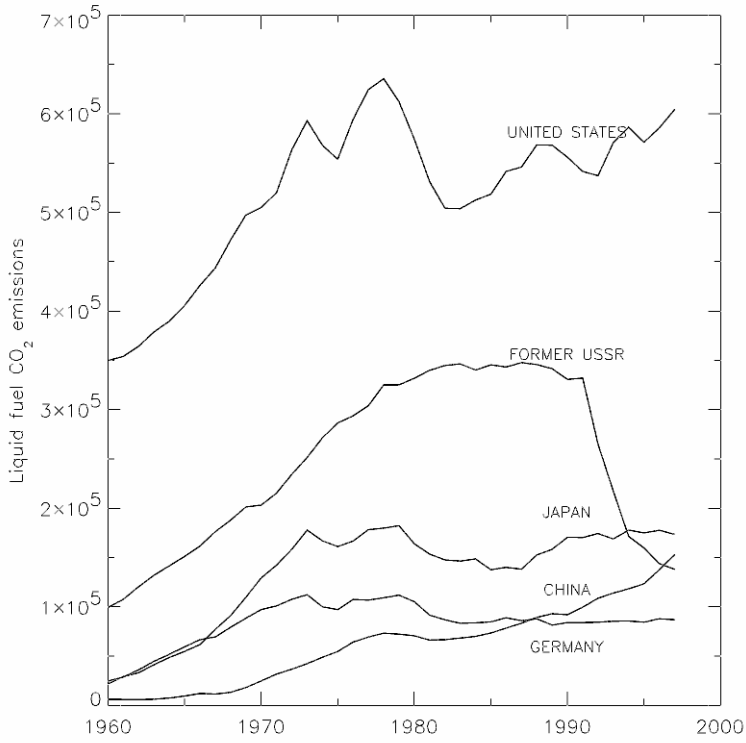

Figure 3: Liquid fuel CO_2 emission trends for the 5 greatest emitting countries (from CDIAC). Unit: MtC/year.

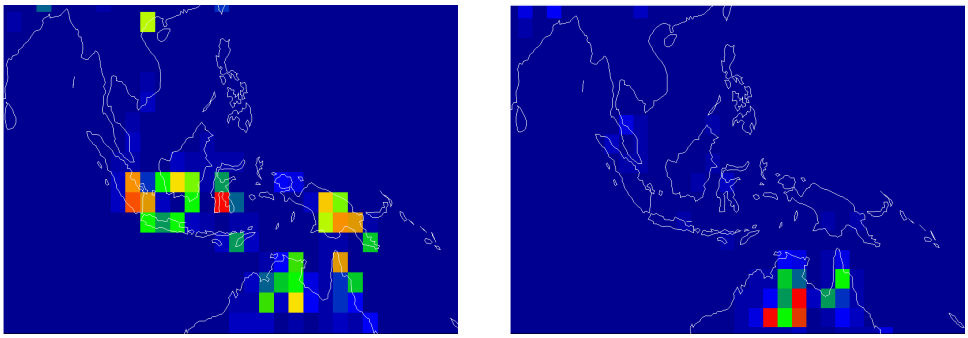

Figure 4: Qualitative illustration of emission fluxes from biomass burning in Indonesia for October 1997 (left) and October 2000 (right). These emissions were derived by scaling the climatological inventory of the MOZART model with normalised monthly mean fire counts from the ATSR satellite.

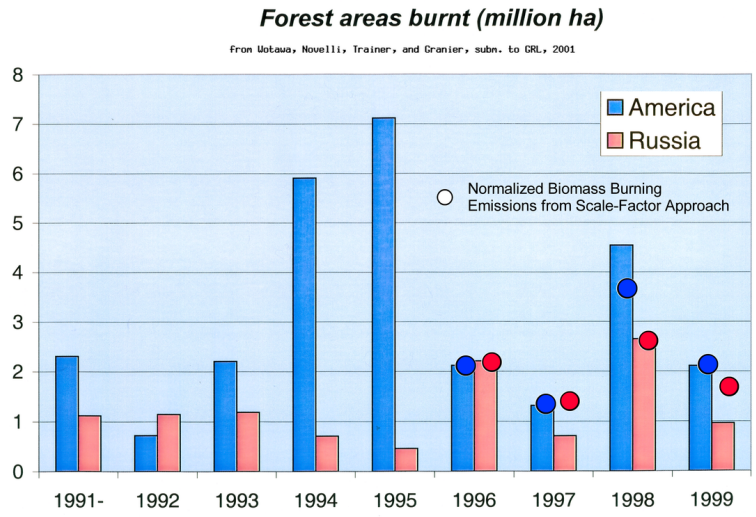

Figure 5: Interannual variability of burnt area from boreal forest fires in North America and in the Russian Federation (from Wotowa et al., 2001) and superimposed normalized emission fluxes for these regions derived from the ATSR fire count scale factor approach.

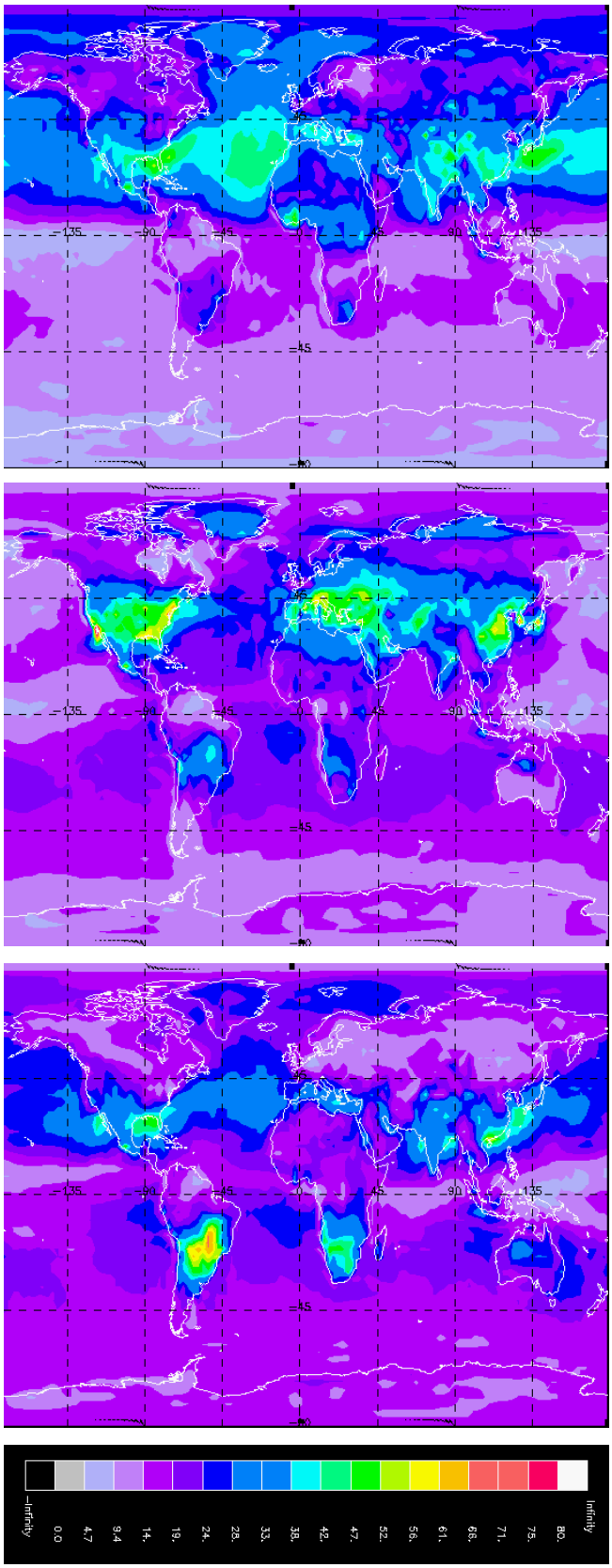

Figure 6: Monthly mean surface ozone concentrations for 1990 computed from the MOZART 2 model for April (top), July (center), and October (bottom). Colour scale in ppb.

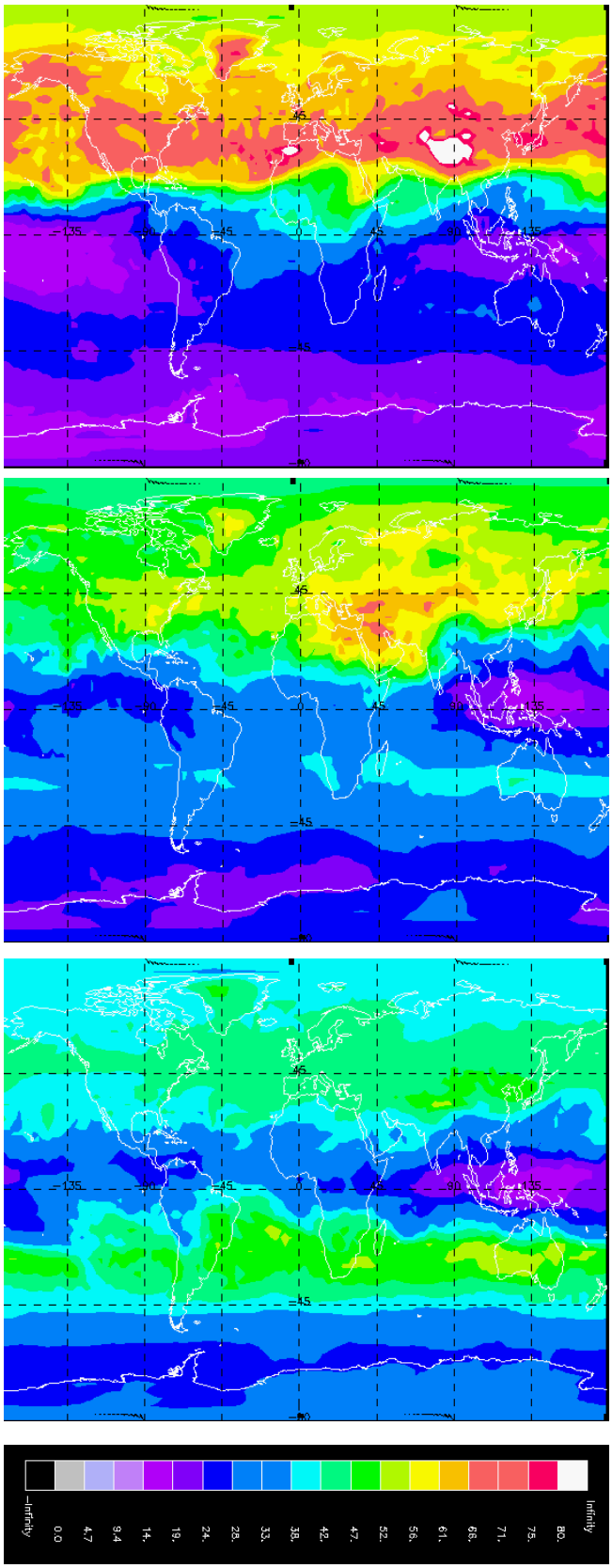

Figure 7: Monthly mean 500 hPa ozone concentrations for 1990 computed from the MOZART 2 model for April (top), July (center), and October (bottom). Colour scale in ppb.

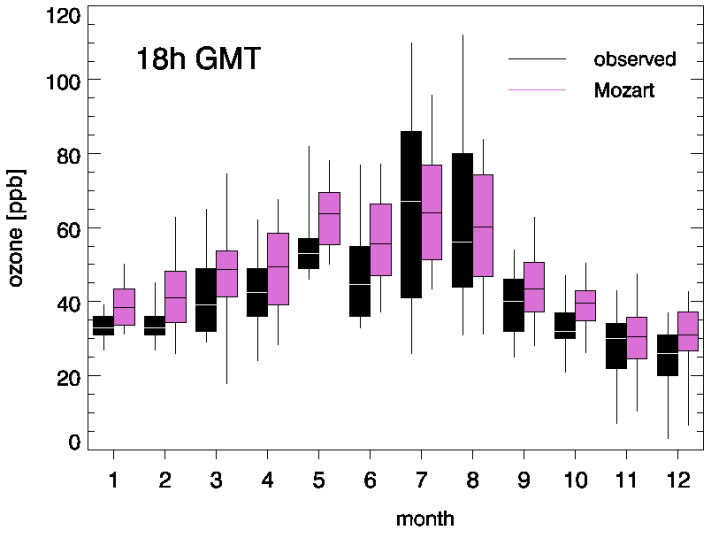

Figure 8: Monthly statistics of ozone concentrations observed at Schauinsland for 1990 and statistics of the MOZART 2 results for the 6−hour interval from 12h−18h GMT. Horizontal lines deonte the median concentration, boxes span the central 50%, and vertical lines cover the central 90% of the data.

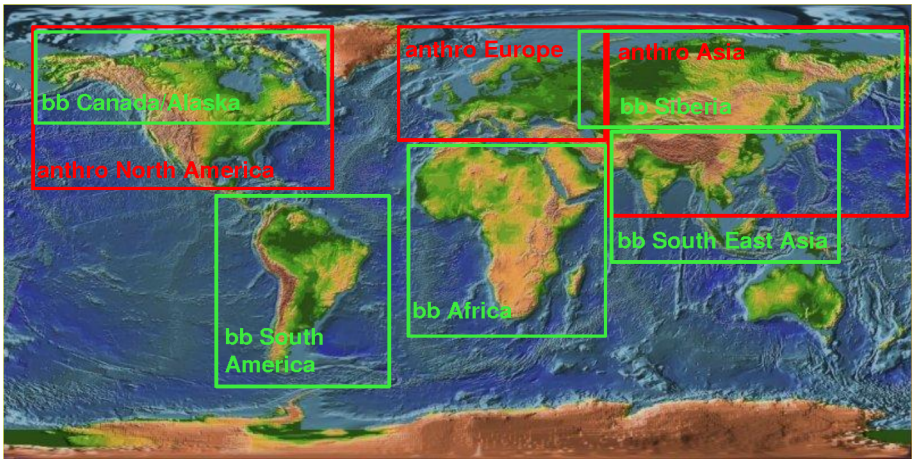

Figure 9: Region boundaries for the tagged CO tracer simulations with the ECHAM−5 model. Fossil fuel combustion emission regions are marked red, those from biomass burning are marked in green.

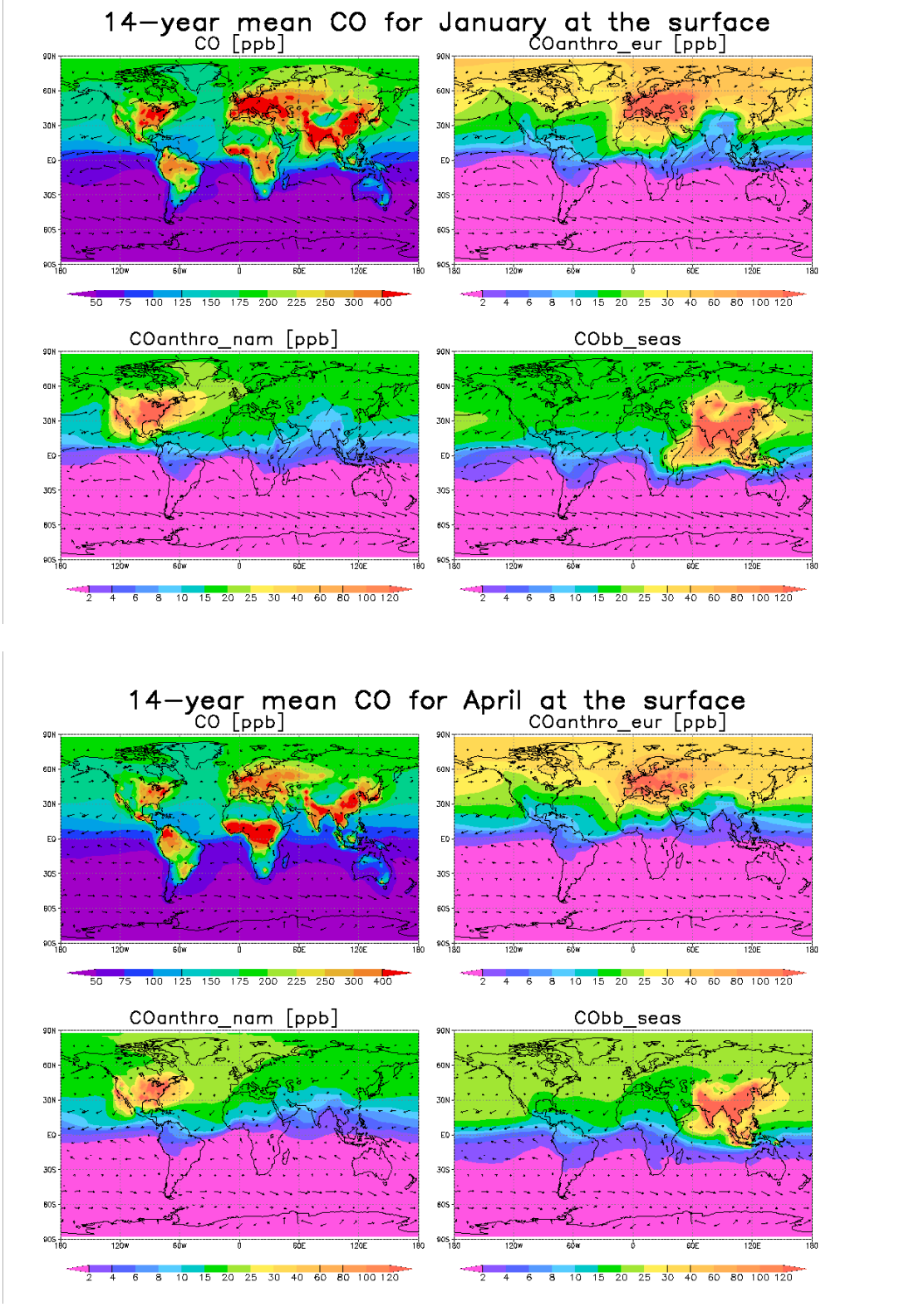

Figure 10: 14−year average surface concentrations of CO from the ECHAM tagged tracer simulations for January (top) and April (bottom). Each panel shows the total CO concentration (upper left), the CO contribution from fossil fuel combustion sources in Europe (upper right), the CO contribution from fossil fuel combustion sources in North America (lower left), and the CO contribution from biomass burning emissions in South East Asia (lower right). Note the different colour scales for total CO and the others.

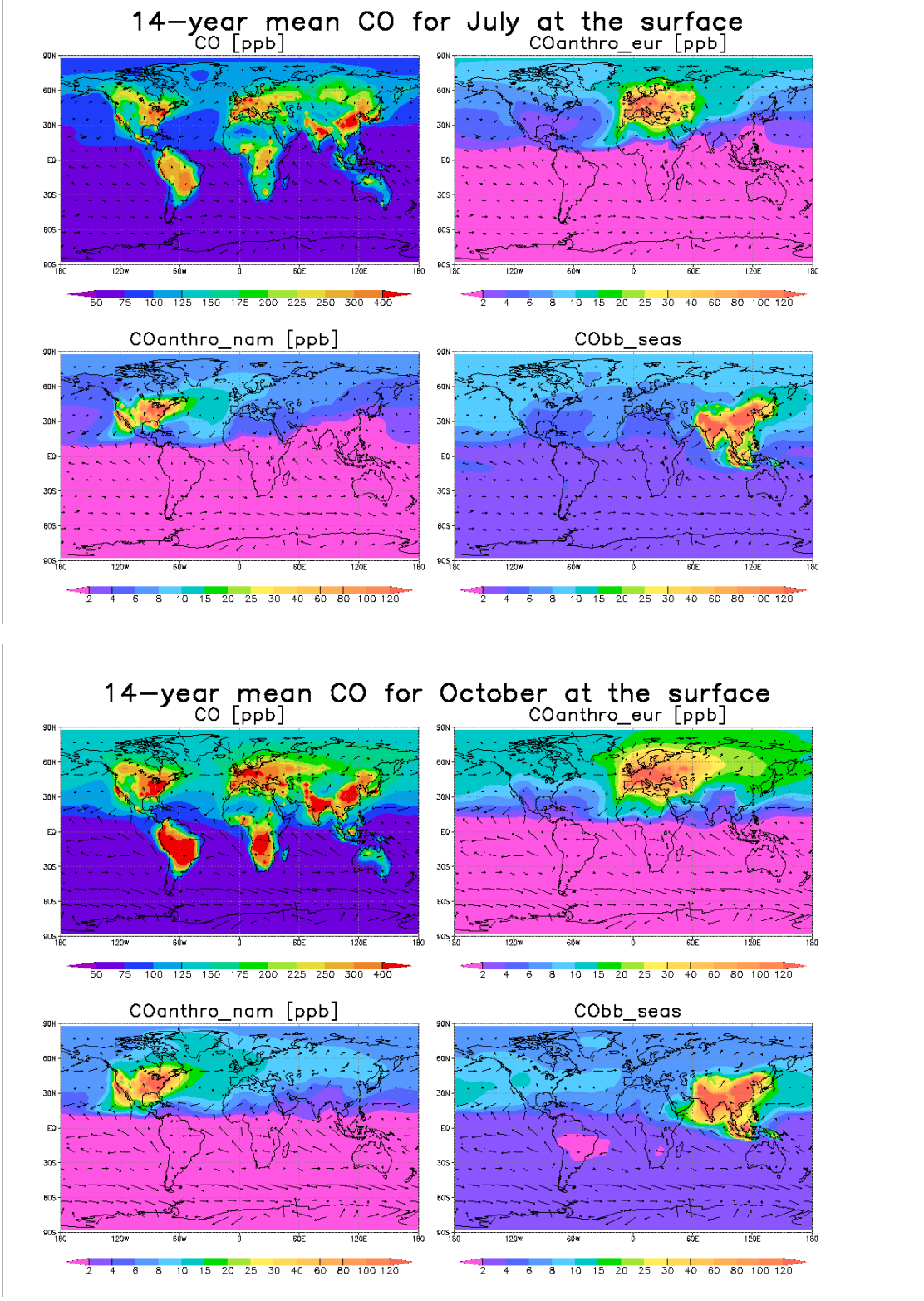

Figure 11: 14−year average surface concentrations of CO from the ECHAM tagged tracer simulations for July (top) and October (bottom). For explanations, see Figure 10.

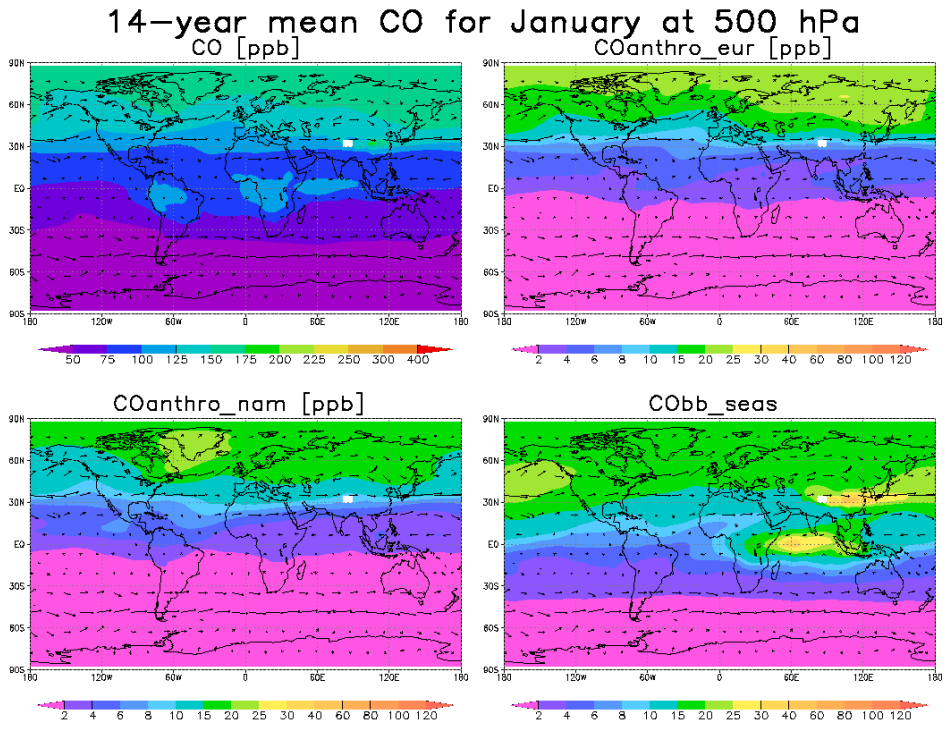

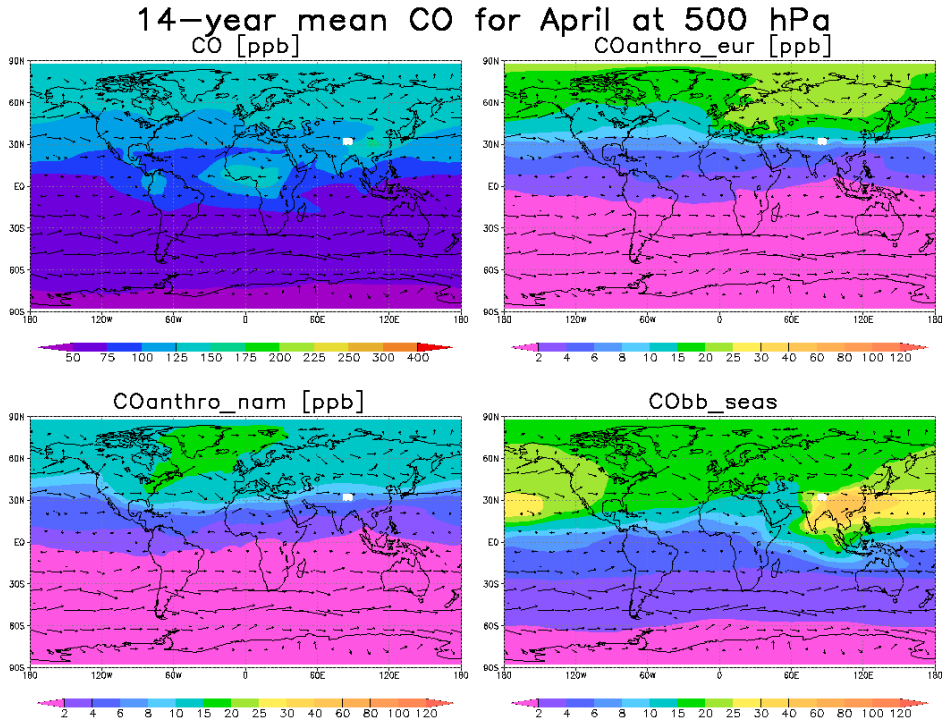

Figure 12: 14−year average concentrations of CO at 500 hPa from the ECHAM tagged tracer simulations for January (top) and April (bottom). For explanations, see Figure 10.

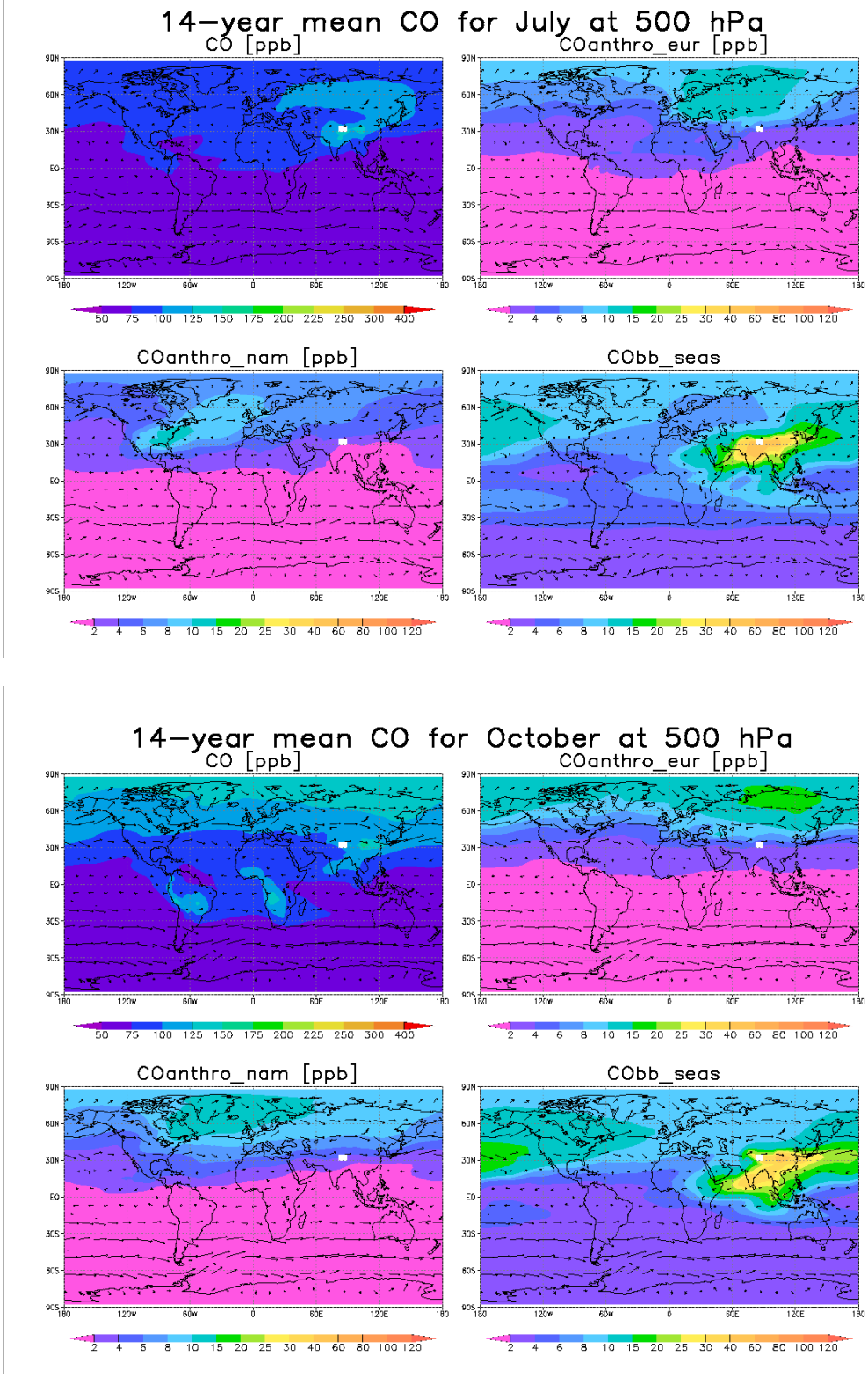

Figure 13: 14−year average concentrations of CO at 500 hPa from the ECHAM tagged tracer simulations for July (top) and October (bottom). For explanations, see Figure 10.

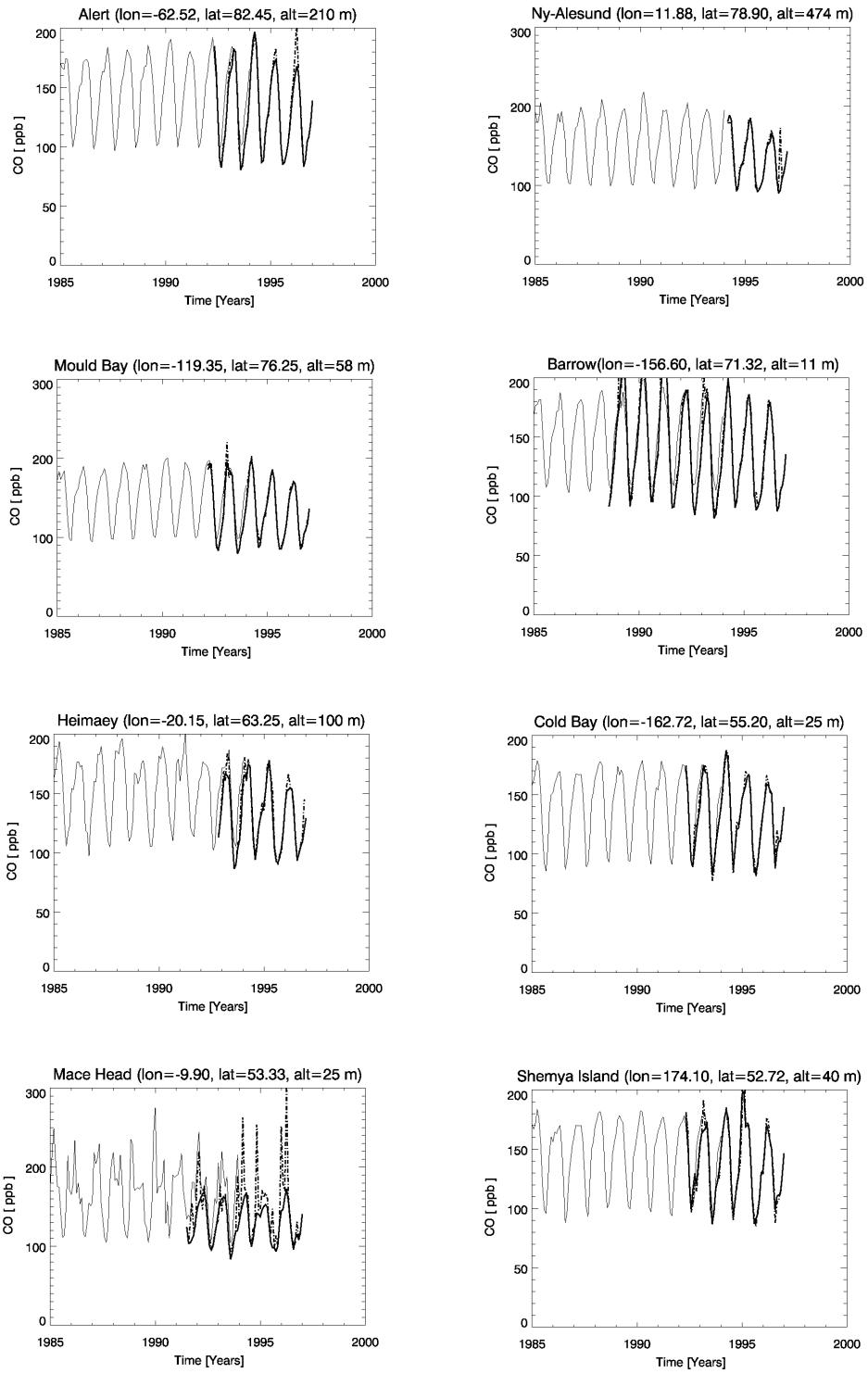

Figure 14: Comparison of ECHAM model results for CO (thin solid line) with CMDL station data (thick solid line). The dashed line denotes a reprocessed CMDL data set where samples that were marked as "polluted" were included in the average. The plots are arranged from north to south.

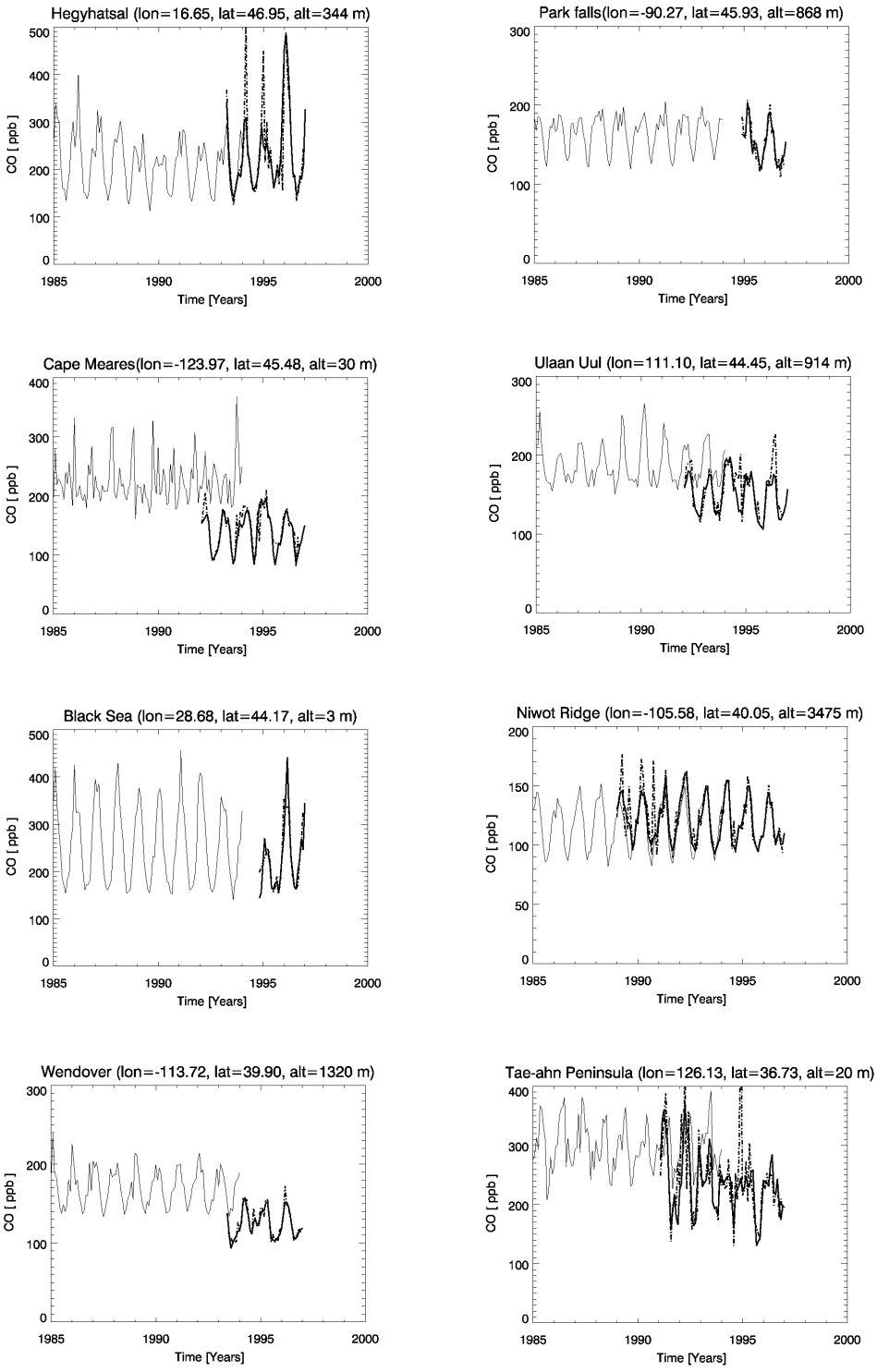

Figure 14 (continued).

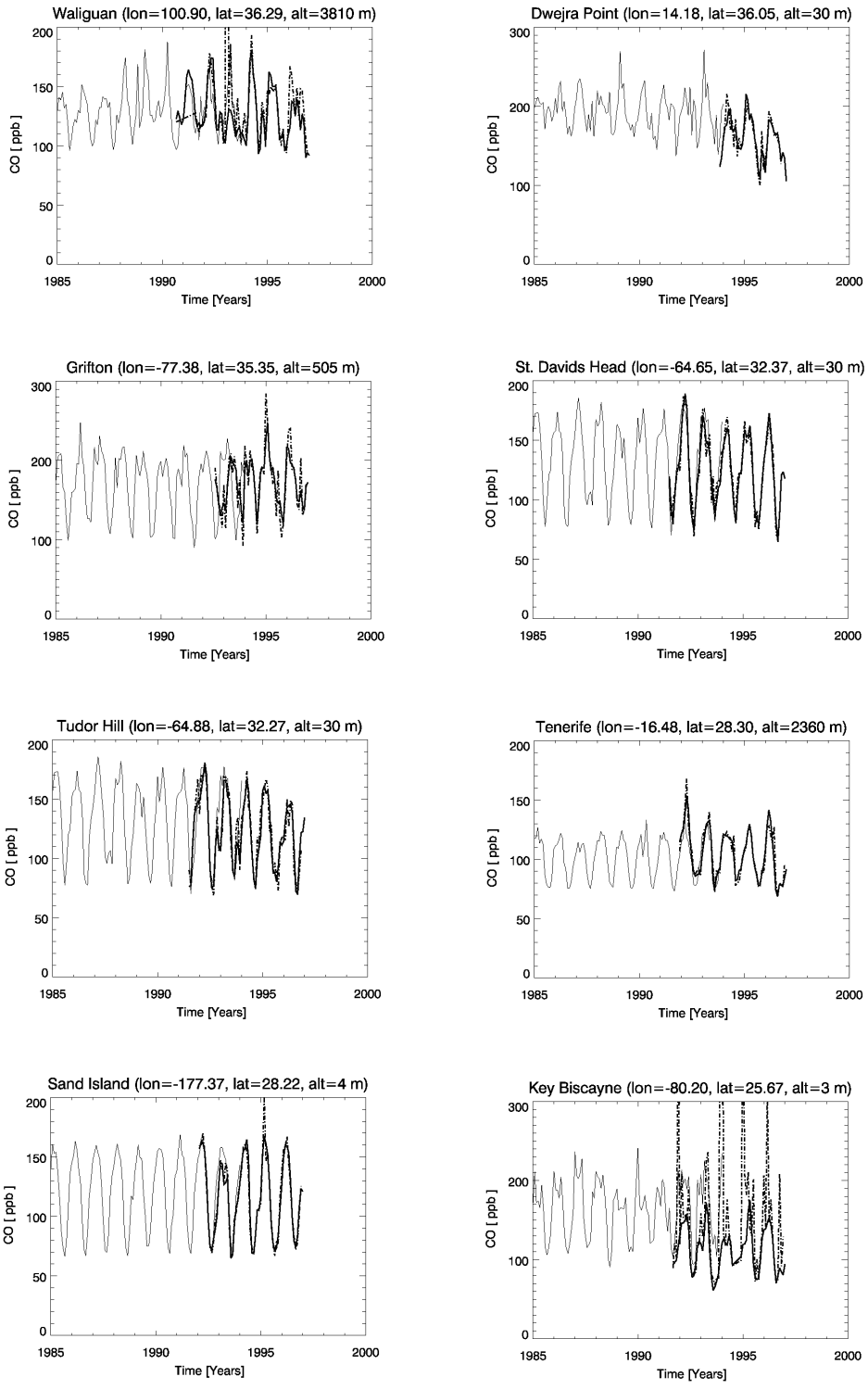

Figure 14 (continued).

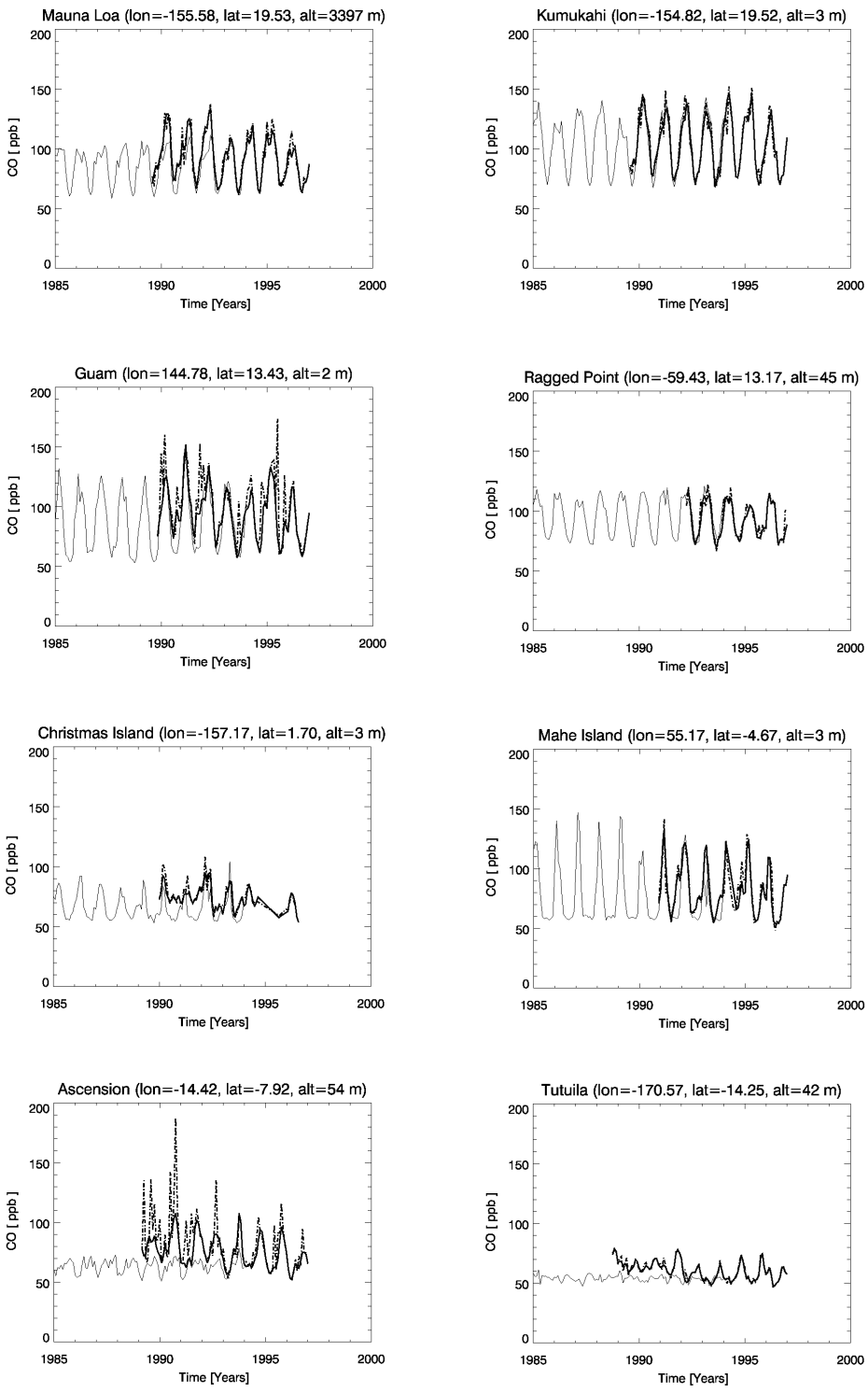

Figure 14 (continued).

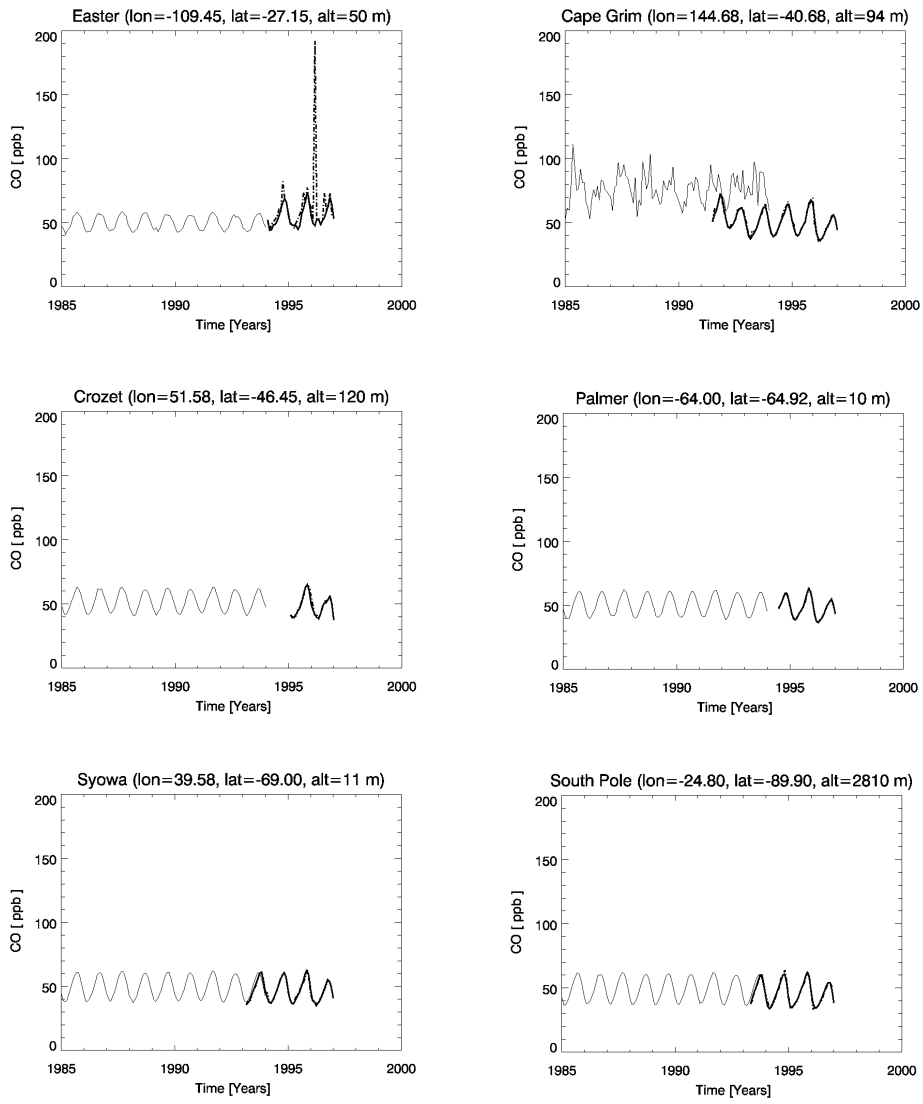

Figure 14 (continued)

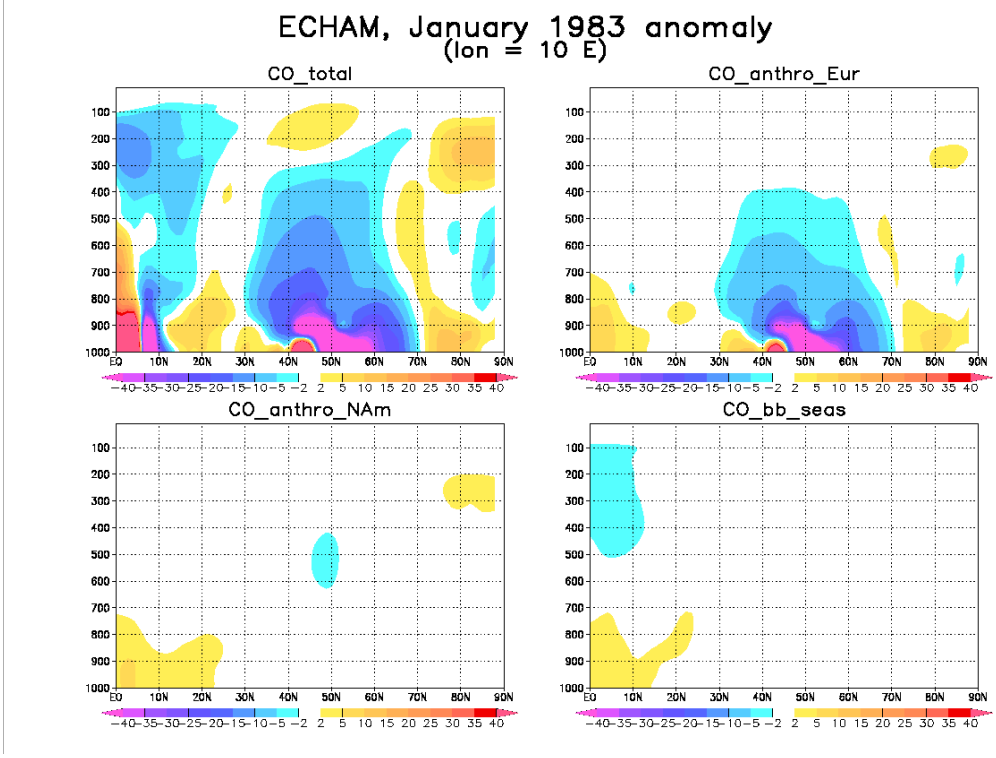

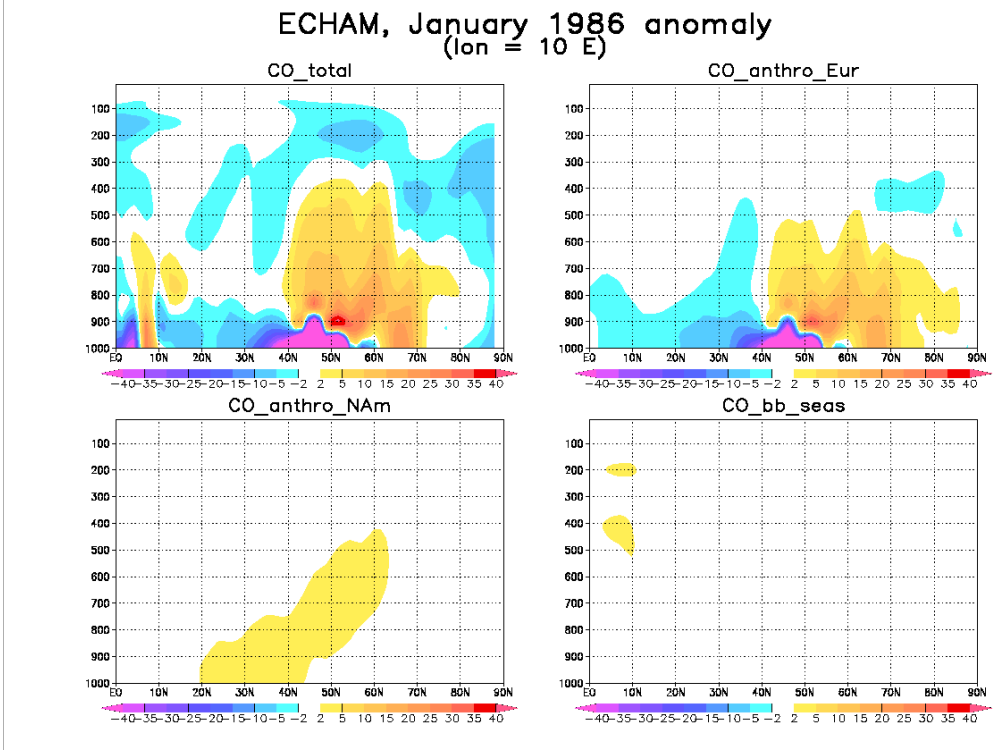

Figure 15: Vertical cross section at 10°E of the CO concentration anomalies (difference between concentration of year X and 14−year mean) for 1983 and 1986 and the month of January. Colour scale in ppb.

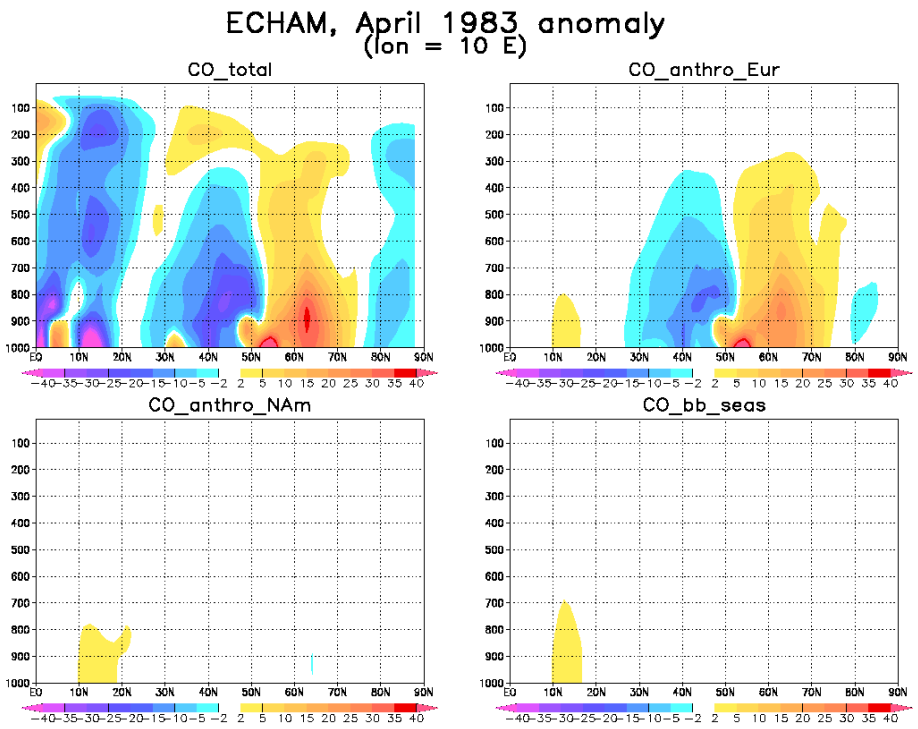

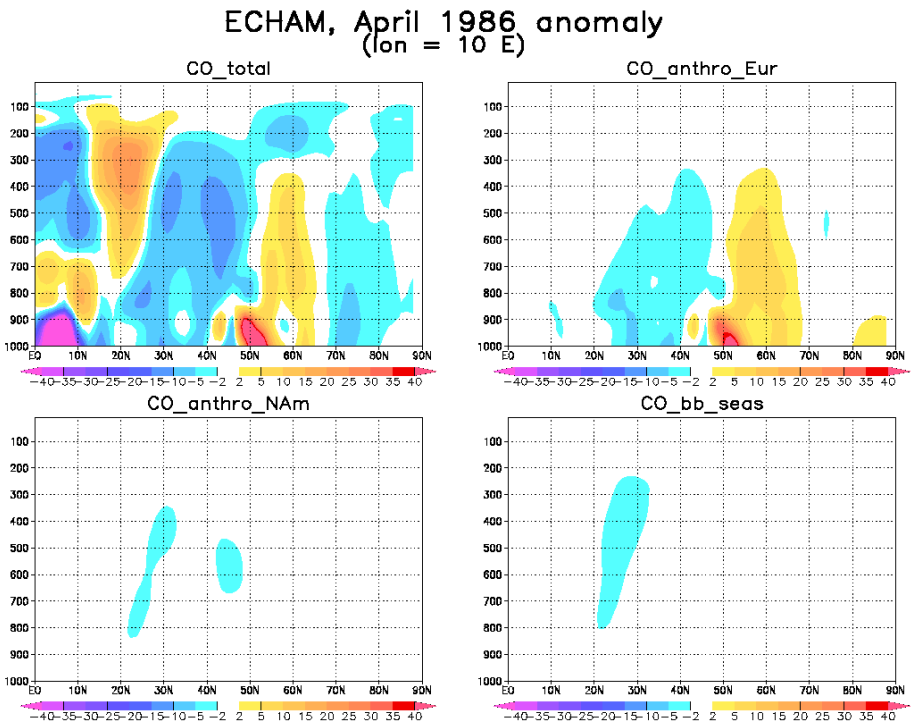

Figure 16: dto. for April.

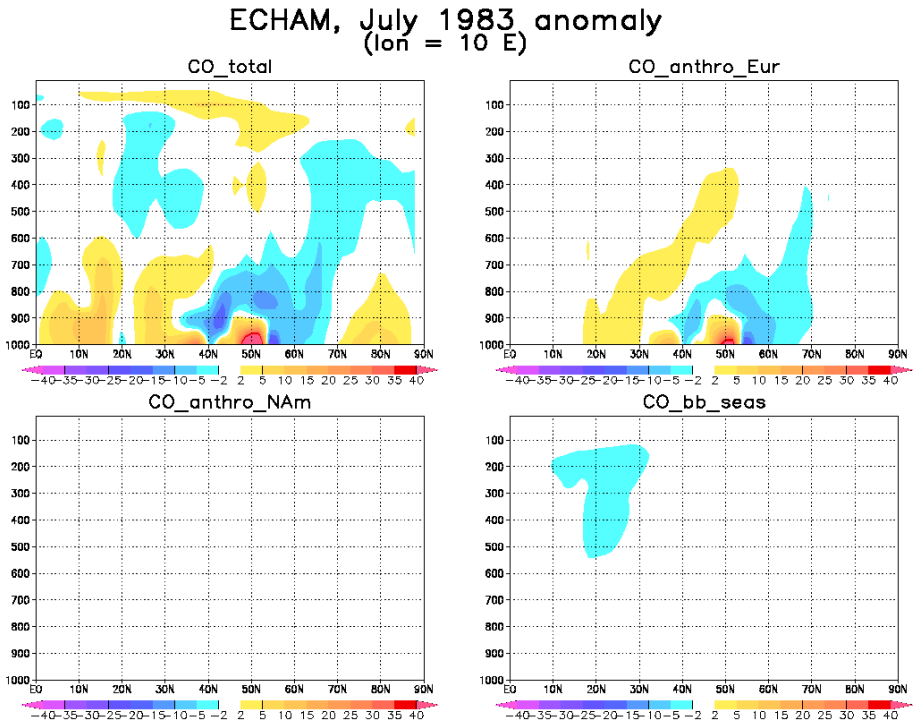

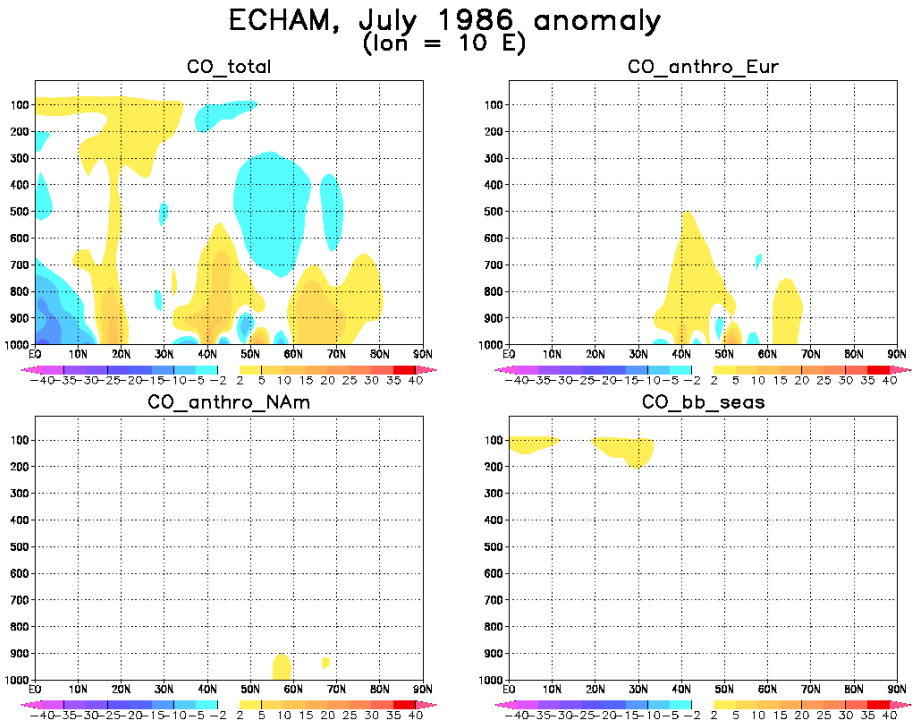

Figure 17: dto. for July.

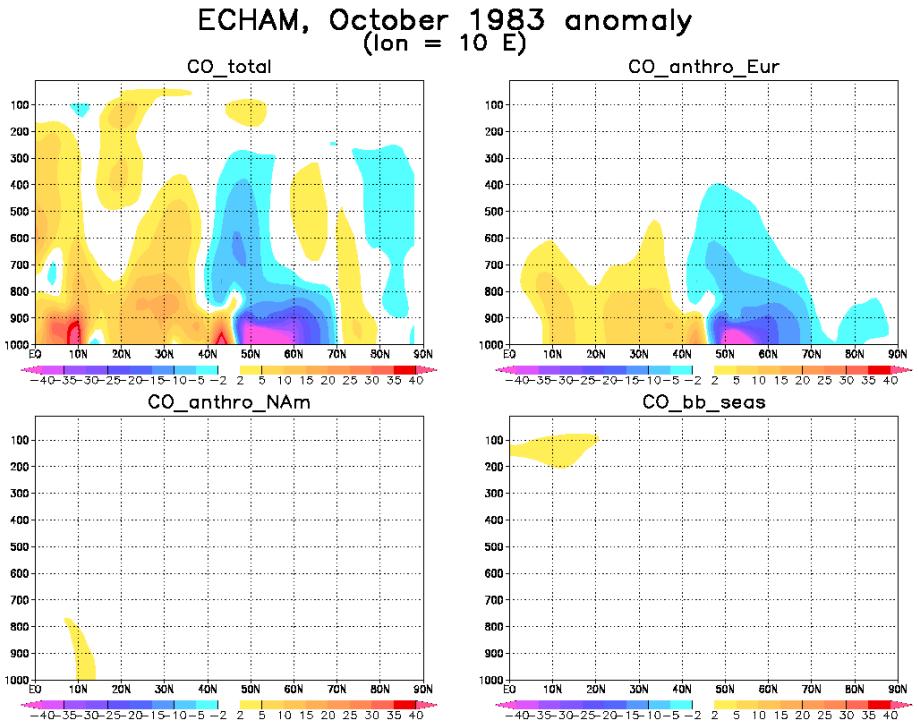

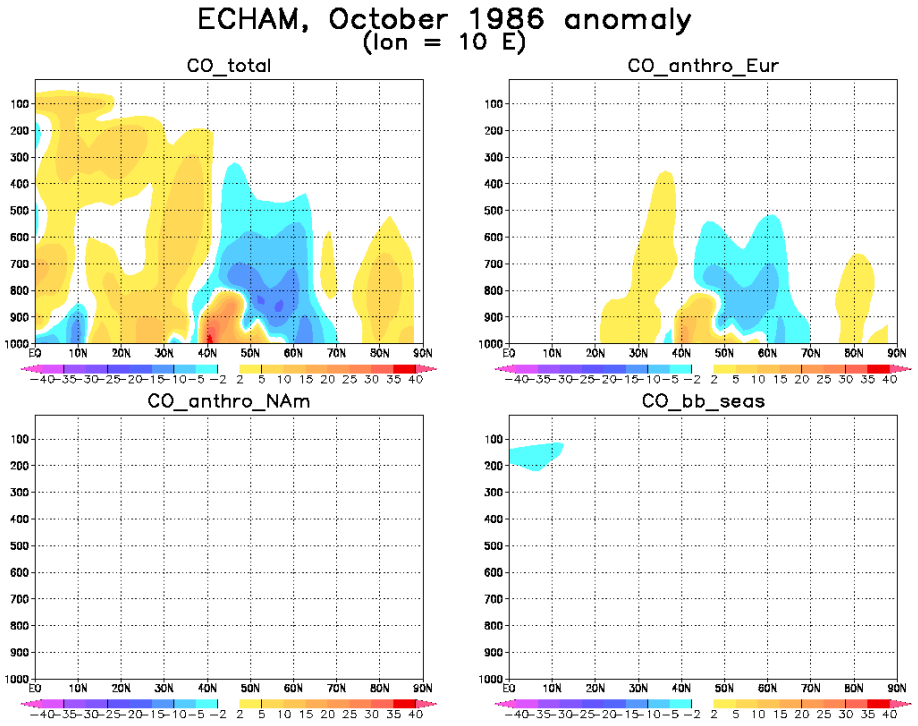

Figure 18: dto. for October.

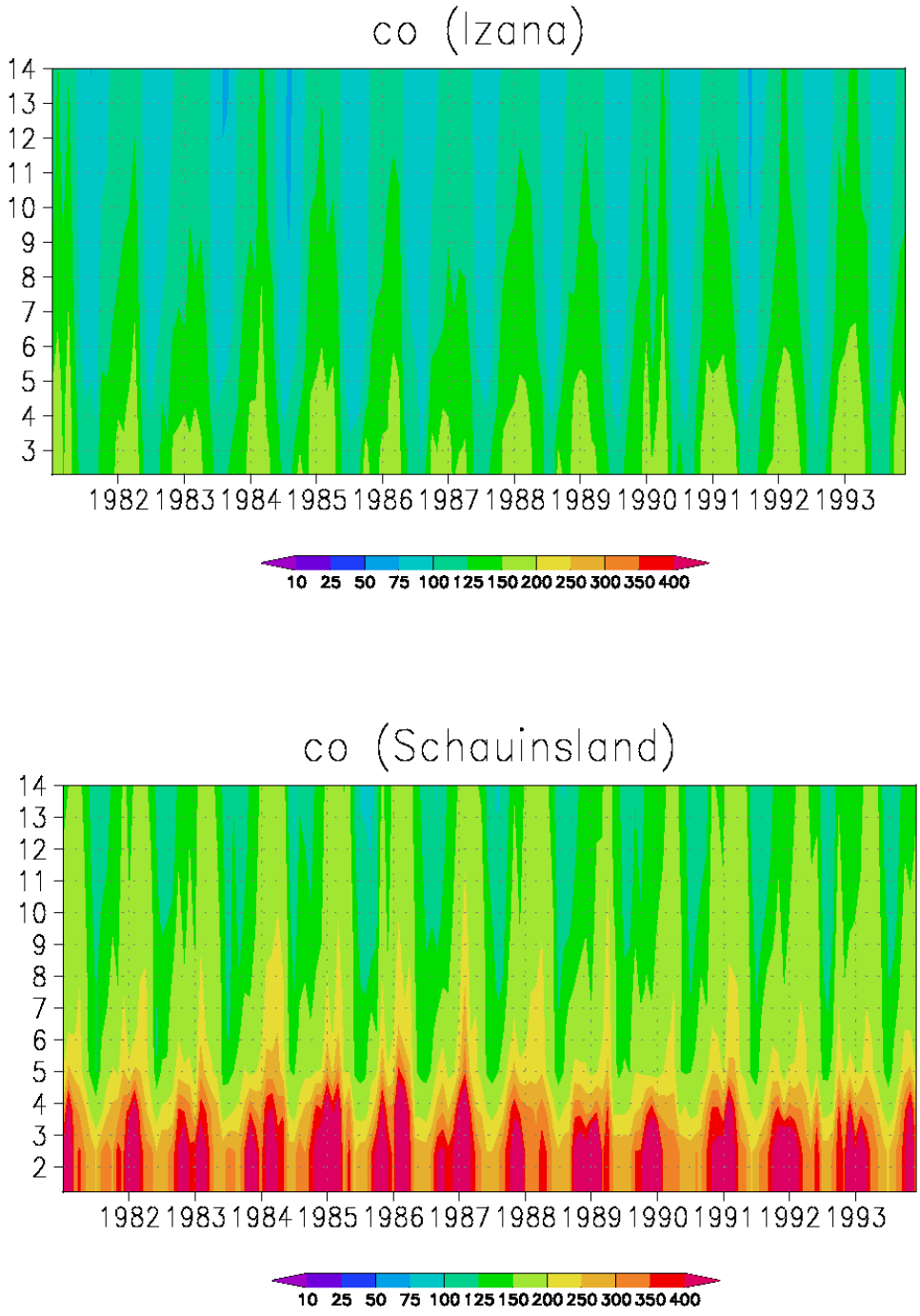

Figure 19: Time−altitude cross sections of the simulated CO concentration for the locations of Izana (top) and Schauinsland (bottom). Colour scale in ppb.

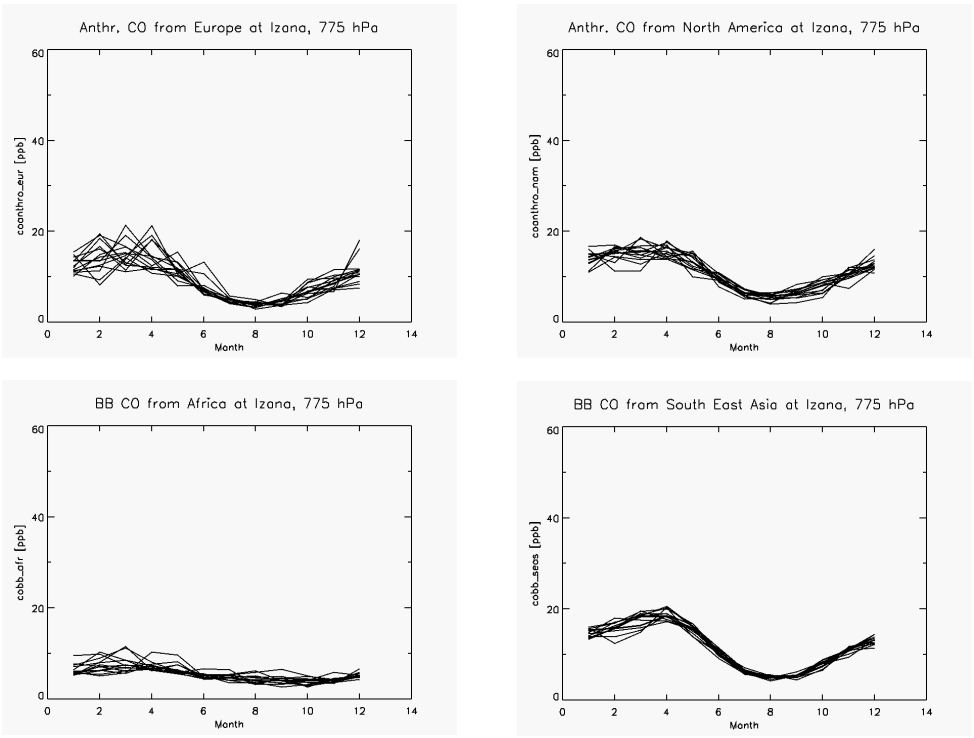

Figure 20: Seasonal variation and interannual variability for the four dominant CO tracers at the Izana station for model level 775 hPa.

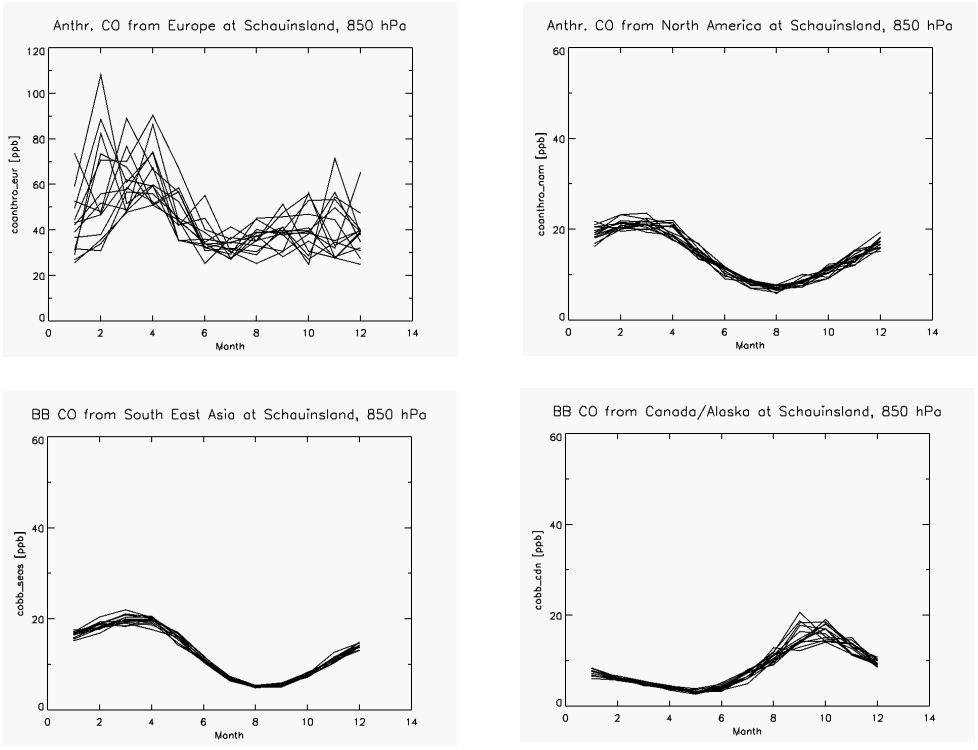

Figure 21: dto. for Schauinsland at 850 hPa.

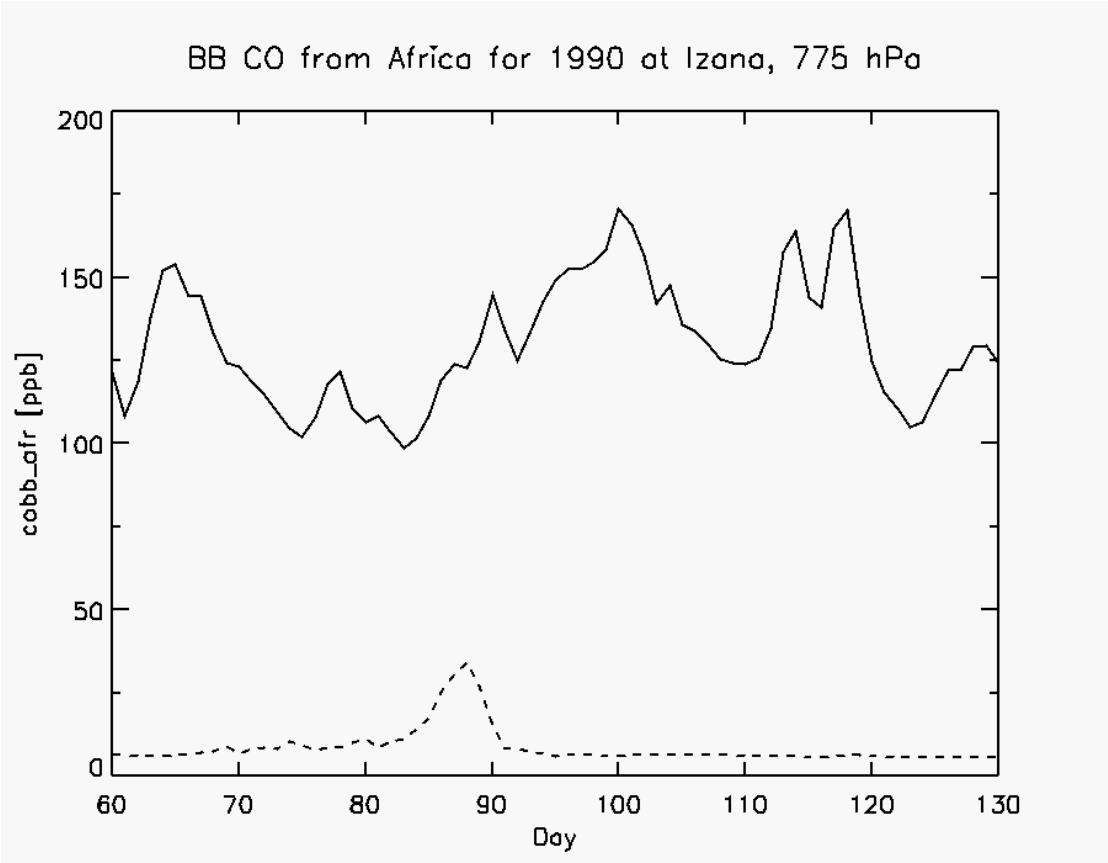

Figure 22: Diurnal average CO concentration (solid line) and contribution of CO from African biomass burning (dashed line) at Izana for a period in March 1990.